Electrochemical and Structural Properties of Organic Carbon based Counter Electrode for Dye Sensitized Solar Cells

By

Syed Kazim Murtaza

Reg # 00000277275

Session 2018-20

Supervised by

Dr. Sehar Shakir

U.S.– Pakistan Center for Advanced Studies in Energy (USPCAS-E)

National University of Sciences and Technology (NUST)

H-12, Islamabad 44000, Pakistan

August 2022

Electrochemical and Structural Properties of Organic Carbon based Counter Electrode for Dye Sensitized Solar Cells

By

Syed Kazim Murtaza

Reg # 00000277275

Session 2018-20

Supervised by

Dr. Sehar Shakir

A Thesis Submitted to U.S.-Pakistan Center for Advanced Studies in Energy

partial fulfillment of the requirements for the degree of

Master of Science in

ENERGY SYSTEMS ENGINEERING

U.S.– Pakistan Center for Advanced Studies in Energy (USPCAS-E)

National University of Sciences and Technology (NUST)

H-12, Islamabad 44000, Pakistan

August 2022

THESIS ACCEPTANCE CERTIFICATE

Certified that final copy of MS/MPhil thesis written by **Mr. Syed Kazim Murtaza** (Registration No. **00000277275**), of U.S.-Pakistan Center for Advanced Studies in Energy has been vetted by undersigned, found complete in all respects as per NUST Statues/Regulations, is within the similarity indices limit and is accepted as partial fulfillment for the award of MS/MPhil degree. It is further certified that necessary amendments as pointed out by GEC members of the scholar have also been incorporated in the said thesis.

Signature: _____

Supervisor: Dr. Sehar Shakir

Date:_____

Signature: _____

HOD-ESE: Dr. Rabia Liaquat

Date:_____

Signature: _____

Principal: Prof. Dr. Adeel Waqas

Date:_____

Certificate

This is to certify that work in this thesis has been carried out by **Mr. Syed Kazim Murtaza** and completed under my supervision in Advanced Energy Material Lab laboratory, US-Pakistan Center for Advanced Studies in Energy (USPCAS-E), National University of Sciences and Technology, H-12, Islamabad, Pakistan.

Supervisor: _____

Dr. Sehar Shakir
USPCAS-E
NUST, Islamabad

GEC Member 1: _____

Dr. Asif Hussain Khoja
USPCAS-E
NUST, Islamabad

GEC Member 2: _____

Dr. Mustafa Anwar
USPCAS-E
NUST, Islamabad

GEC Member 3: _____

Dr. Mariam Mahmood
USPCAS-E
NUST, Islamabad

HOD-ESE: _____

Dr. Rabia Liaquat
USPCAS-E
NUST, Islamabad

Principal: _____

Prof Dr. Adeel Waqas
USPCAS-E
NUST, Islamabad

DEDICATION

This thesis is dedicated to my loving Parents, Family, Friends, Teachers.

Acknowledgment

First and foremost, all praise to **Allah Almighty**, The Most Beneficent, and The Most Merciful, who gave me strength to achieve this goal. Second i want to give my genuine gratitude to my supervisor Dr. Sehar Shakir for her selfless guidance, tremendous support, and sharing a wealth of knowledge during my research work. I really appreciate her valuable critiques, comments, and suggestion during the thesis write-up. I believe that this thesis write-up would not have been possible to complete without her.

I also want to thank my graduate examination committee (GEC) members, Dr. Asif Hussain Khoja, Dr. Mustafa Anwar, and Dr. Mariam Mahmood who honored my committee presence and for having a major contribution in improving this thesis work.

I appreciate the support of faculty and lab engineers at USPCAS-E for all things that facilitated the research work and assistance every step of the way. I also indebt my lab fellows for their continuous help during the research.

Finally, and most importantly, I must express my very profound gratitude to my family who encouraged and facilitated me at every phase of my personal and academic life.

Thank You

Syed Kazim Murtaza

Abstract

Dye sensitized solar cells (DSSC) are the important class of solar cells that are currently gaining the attention of scientists and researchers. The replacement of platinum based counter electrode with activated carbon can make them cost effect for different energy storage and conversion processes. In this regard, the synthesis of activated carbon from biomass is of current interest towards energy sustainability. Carbonization process largely influence the properties of biomass derived activated carbon. This study encompasses the preparation of activated carbon with extremely large surface area and high porosity from hemp using chemical activation process. Initially the hemp leaves were carbonized at 750℃ followed by the activation using H_2O_2. Carbonaceous counter electrode containing Hemp activated carbon (HAC) was then fabricated by Doctor Blade coating Technique on FTO glass substrate. Preparation of photoanode and ultimately assembling of DSSC were carried out. Different characterization techniques like XRD, FTIR, SEM, Raman Spectroscopy and Cyclic Voltammetry were used. The surface morphology was examined by SEM and it shows the development of regular porous structure. The surface functional groups like –OH, -COOH, -C=C/C-C were confirmed by FTIR. The crystalline and graphite nature of HAC was determined by Raman spectroscopy and X-ray diffraction technique. This study offers an environmental friendly procedure for the massive production of activated carbon from hemp.

Keywords: *Dye Sensitized Solar Cell, solar cell, hemp activated carbon, XRD, SEM, Raman*

Table of Contents

List of Figures

List of Tables

List of Abbreviations

TFEC	Total final energy consumption
GHGs	Greenhouse gas emissions
CE	Counter electrode
DSSC	Dye sensitized solar cell
ITO	Indium doped tin oxide
FTO	Fluorine doped tin oxide
CVD	Chemical vapor deposition
XRD	X-ray diffraction
SEM	Scanning electron microscope
CV	Cyclic voltammetry
C-TiO_2	Carbon-doped titania
PV	Photovoltaic
CO_2	Carbon dioxide

List of Publications

Conference Paper: Syed Kazim Murtaza, Faisal Abbas, Syeda Farah Naz, Mustafa Anwar, Asif Hussain Khoja, Sehar Shakir*, “Electrochemical and Structural Properties of Organic Carbon based Counter Electrode for Dye Sensitized Solar Cells”, International Conference on Mechatronic Systems and Robots, **Status: Submitted**

Chapter 1: Introduction

1.1 Renewable Energy Technologies and Energy Demand

1.1.1 Energy and Economy

The economic stability of a country is dependent upon the pace of technological and industrial development which provides different employment opportunities and growth in the gross domestic product of that country and hence feed the masses. This technological and industrial development is solely dependent upon the availability of adequate, reliable, and sustainable energy. Thus, economic stability is directly linked with energy availability. Energy consumption is considered an indicator of how much economic growth is occurring. As a result, there is always an increase in demand for sustainable energy. Advanced countries like China and the United States of America (USA), in addition to fossil fuel-based power plants, have built hundreds of hydro-dams, nuclear power plants, and renewable energy equipment. Still, these advanced nations are looking for new methods (e.g., nuclear fusion) of harnessing energy to meet the predicted needs of future generations.

1.1.2 Increasing Energy Demand

Demand of global energy will increase by 4.6% after lowered energy demand due to the Covid-19 pandemic as per International Energy Agency (IEA) [1]. Furthermore, demand for fossil fuels in the year 2021 will likely grow at exponential trends. Just for coal, demand alone is predicted to increase by 60% while for oil, global demand will be around 3% in 2019 [2]. Fossil fuels (Coal, Natural Gas, Furnace Oil, etc.) are predominantly used for energy production. Of World's total energy production, almost 84.3% is obtained via fossil fuels [3]. Fossil fuels contain compounds primarily made up of carbon and hydrogen. They are formed due to the decomposition of dead plants and animals buried deep under the earth's crust due to high temperature and pressure. As far as global primary consumption by the source is concerned, Oil contributes 33.1% to global energy followed by coal and gas with 27% and 24.3% respectively [4]. Over the past decades, the population is increasing at an exponential rate and thus associated with a rise in population per capita energy usage. An estimated increase of 40% rise in energy demand has already occurred due to the increase in the population [5]. Another important factor is the different energy demands between developed and developing/under-developed countries

with the latter having more. The cumulative energy consumption for all regions is predicted to increase to 762 exajoules (212,201 Terawatts) by the year 2030 [6]. Thus, to meet such huge demand, the world is overly reliant on fossil fuel resources.

1.1.3 Conventional Energy Resources

For the first time in 1973, the Oil Crisis showed how much dependent was the entire world on fossil fuels [7]. It was not only a manifestation of a world without fossil fuels but also a wake-up call for researchers to find alternate methods of harnessing energy if fossil fuels are depleted. Even though new oil and gas reserves are found now and then, it is evident that the world will eventually run out of fossil fuels. Earth has nearly 1.688 trillion barrels of crude and at the current rate of extraction, it will last approximately 53.3 years [8]. But during the last ten years, proven reserves have increased by 27%, or 350 billion barrels. An additional 900 million barrels of oil were detected in Russia and approximately 800 million barrels in Venezuela. This amount may increase in the future as the world is tapping into the domain of shale oil and gas reserves which have remained untouched previously. These facts indicate that the world may buy some time with such a fractional increase in oil and gas; however, pollution and greenhouse gas (GHG) emissions are a serious concern associated with fossil fuels.

1.1.4 Pollution and GHG Emissions

In addition to scarcity, one other downfall of fossil fuels is the associated pollution and GHG emissions. As a result of the burning of fossil fuels, different harmful gases and particulate matter are released into the atmosphere as pollutants. Environmental Protection Agency (EPA) has defined certain gases and particulate matter (PM) as pollutants that have acute, chronic, or carcinogenic effects on human health. These pollutants are termed Criteria Air Pollutants and included Carbon Monoxide (CO), particulate matter (PM), Nitrogen Dioxide (NO_2), Lead (Pb), Sulfur Dioxide (SO_2), Ground-Level Ozone(O_3) etc. These pollutants when present beyond certain levels makes the atmosphere polluted and hence, detrimental to human health and survival [9].

Table 1.1 Air Quality Standards for Criteria Air Pollutants, Averaging Time, and Concentration

Air Quality Standards for Criteria Air Pollutants			
Sr. no	**Pollutants**	**Averaging Time**	**Concentration**
1.	CO	08 hour	8 ppmv (10mg/m3)
		01 hour	36 ppmv (40mg/m3)
2.	Pb	Max Quarterly Average	0.15 μg/m3
3.	NO_2	National Arithmetic Mean	0.0533 ppmv
4.	Ozone	1-hour Average	0.121 ppmv
		8-hour average	0.08 ppmv
5.	PM 10	Annual Arithmetic Mean	49 μg/m3
		24-hour Average	149 μg/m3
6.	PM 2.5	Annual Mean	65 μg/m3
		24-hour	15 μg/m3
7.	SO_2	Annual Mean	80 μg/m3
		24 hour	360 μg/m3

In addition to harmful hazardous effects on human health, another associated danger is increased climate change. This happens due to an increase in GHG emissions. Earth's natural atmosphere is like a big greenhouse gas shed to control the temperature of the biosphere which is necessary for the survival of life. Different gases have different absorption capacities for incoming ultraviolet rays and outgoing infrared rays. The potential of these gases to cause global warming when comparing it with the amount of global warming caused by Carbon is known as Global Warming Potential (GWP); thus, the more the GWP, the higher will be global warming caused by these gases. Due to human activities, the volume of these gases has increased in the

atmosphere causing a massive increase in global warming and hence the rise of global temperature. In addition to the gases mentioned above, water vapor, carbon dioxide, methane,

Table 1.2 Green House Gases, Atmospheric Concentrations, Average Lifetime, and GWP

Green House Gases, Atmospheric Concentration, Average Lifetime, and GWP					
Sr #	**GHG**	**Pre-Industrial Concentration**	**Concentration in 2018**	**Average Lifetime (Yrs)**	**GWP**
1	CO2	280 ppmv*	449 ppmv	50-200	1
2	Methane CH4	715 ppbv*	1700 ppmv	10-15	21
3	Nitrous Oxide (N2O)	270 ppbv	320 ppmv	115-145	310
4	CFCs	0	503 pptv*	102	125-152
5	HCFCs	0	105 pptv	13	123
6	Perfluorocarbon (CF4)	0	110 pptv	50,000	6500
7	Sulphur Hexa-Fluoride (SF6)	0	72 pptv	1000	23900

pptv – parts per trillion by volume
ppbv – parts per billion by volume
ppmv – parts per million by volume

Chlorofluorocarbons (CFCs), and various other gases are included to be GHGs. Furthermore, some of these gases can remain in the atmosphere for hundreds of years. So, during all that time, they will further add to the deteriorating situation.

1.1.5 Tackling Energy Insecurity and Mitigation of Detrimental Climate Effects

To tackle the challenge of energy insecurity, scarcity of conventional resources, and mitigation of climate change, three main solutions have been proposed (i) Nuclear Fusion/Fission power, (ii) Carbon Capturing and Sequestering while burning fossil fuels, and (iii) Investing in renewable energy generation. Both nuclear fusion and fission are carbon-free energy generation processes [10]. However, nuclear fission involves the decomposition of Uranium-235 which is a scarce element and is very difficult to secure. Furthermore, disposing of nuclear waste is another troubling feature because of its very high toxicity and prolonged half-life. On the other hand, nuclear fusion involves the fusion of different elements thus generating huge energy during the process; however, nuclear fusion requires very high temperature and pressure conditions. Researchers are focused on achieving suitable conditions for nuclear fusion to happen. In addition to nuclear power production, decarbonizing i.e., carbon capture and the sequester is another option. However, the main challenges for carbon sequestration are the costs of carbon dioxide separation, capture, and finally making safe and economical dumping spots (sinks) [11]. Thus, investing in renewable energy sources seems like the more suitable and viable option.

1.1.6 Renewable Energy Technologies

1.1.6.1 Wind Energy

Wind energy is derived from the air through wind turbines. The wind power depends upon the speed of the wind and it is expressed as $P = \frac{1}{2}\rho AV^3$ (P=Power, p=density, A=swept area,V=wind speed) [12]. Hence, with the increase in wind speed, there is an exponential increase in power.

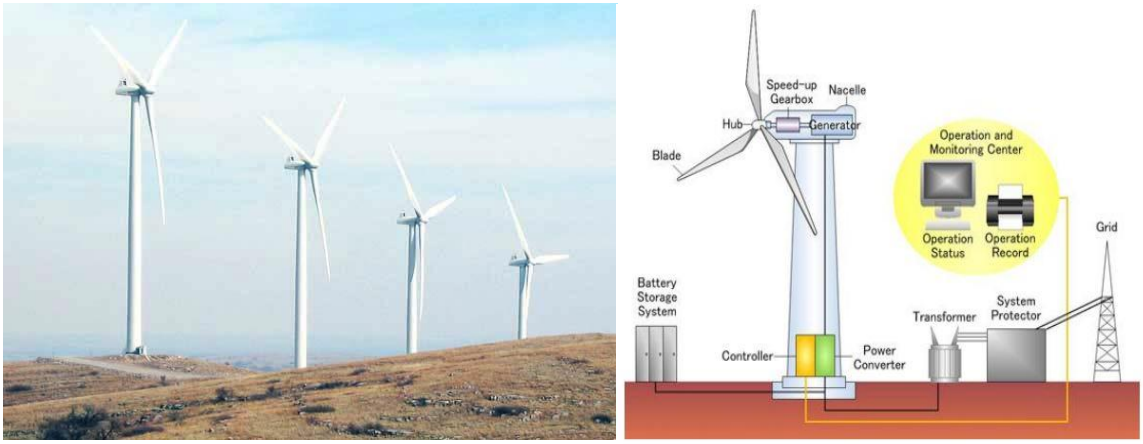

Figure 1-1 Power generation using wind energy

Offshore and high-altitude areas, where wind speed is high and constant, are considered the best locations for wind farm installations. Overcoming all technical and environmental barriers, global wind potential is considered to be 45 times the current electricity demand [13]. In the year 2020, 93 GW of wind power technology was installed with China's contribution of 55% followed by the US (18%), Brazil (2%), and many other countries. As a result, the total worldwide wind power capacity increased to 763GW which will be helpful to avoid 1.1 billion tons of CO_2 globally. Still, it is a very long way from achieving the maximum global potential of 14TW [14].

1.1.6.2 Hydropower

Harnessing energy from falling water or running water is known as hydro-power. This energy can be obtained either by building large water reservoirs/dams and installing water turbines or by putting turbines in the waterway of run-of-the-river systems. This technology is also applied in remote hilly areas to extract the energy of waterfalls. Hundreds of hydroelectric dams have been built in various countries as it is the cheapest source of electricity excluding building costs. China took the lead by building the largest dam, the Three Gorges Dam, having a power generation capacity of 22GW with a water storage capacity of 39 million cubic meters [15]. However, hydropower dams are very expensive to build and have various environmental concerns.

1.1.6.3 Geothermal Energy

The thermal energy found inside Earth's crust is known as geothermal energy. Very high temperature and pressure inside the core and mantle layer cause the rock to melt and transfer this energy to the upper layers through the convective movement of the mantle. At the core-mantle boundary, temperature can reach as high as 4500 ^{0}C [16]. This heat is utilized in running binary cycle power stations, flash steam power stations and dry steam power stations, and. As of 2019, total worldwide power generation capacity from geothermal energy is approximately 15 GW [17]. It can be used both for space heating and power generation, geothermal energy has the potential to meet 5 percent of global demand [18].

1.1.6.4 Biomass and Biofuel

Biomass is material of biological origin obtained from living organisms and is usually plants-based materials. Biomass is either burnt directly to obtain energy utilising the heat produced during burning or by converting indirectly into biofuel [19]. Biomass includes dead leaves, dead trees, wood chips, eucalyptus, sugar cane, hemp, and other plant debris. Using many methods of chemical treatment, plant biomass is converted to glucose from cellulose. This results in the formation of first generation biofuel. It can exist in all three forms i.e. liquid, gas, and solid forms. Bioehtanol and biodiesel falls in catergiry of liquid biofuels whereas biogas is gaseous biofuel. In 2010, types of biofuels provided 2.7% of global transportation fuels [20].

1.1.6.5 Solar Energy

Keeping in view different renewable energy resources, perhaps the most abundant, practical and reliable form of renewable energy is solar energy. Nearly 130,000 TW solar energy hits the surface of earth per annum, thus plenty of energy is available to be utilized. Solar energy can be directly converted to electricity (Photovoltaics), solar to fuel conversion (photochemical water splitting), solar cooling and heating, and solar thermoelectric,. It can also be utilized indirectly i.e., wind to electricity generation using wind turbines, hydropower, and biofuel energy. This study focuses on Photovoltaic cells or PV solar cells which work by converting incident particles of light

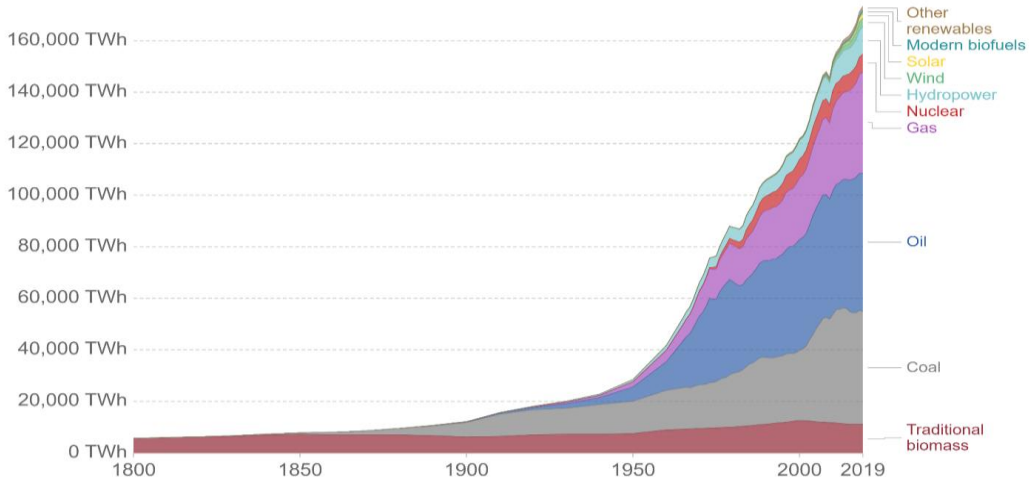

Figure 1-2 Global primary energy consumption by various sources

(photons) into electrical charges directly and providing to external load. Sun energy is the only form of energy that is widespread and even available in the remotest areas of Earth. Thus, using solar cells enable humans to harness energy, whereas providing energy otherwise is an enigmatic task in remote hilly or desert areas. Initially, solar cell technology was very expensive and hence undesirable as energy cost per watt was very high. However, PV researchers have worked a lot in the past decade to find a reasonable ratio of efficiency and effective cost.

1.2 Photovoltaic Technology

Photovoltaics (PV) is the technology that converts incoming solar radiation directly into electric current by using semiconductors. This type of power generation employs several solar panels or modules containing various smaller units having a photovoltaic material. Energy generation by solar photovoltaics is the cleanest renewable energy technology as its operation does not involve any environmental emissions and is hence considered very environement friendly [21]. There are three main stages involved in working of a solar cell; (1) absorption of solar energy, (2) electron-hole pair generation and separation of these two charges, and (3) providing these charges to the load.

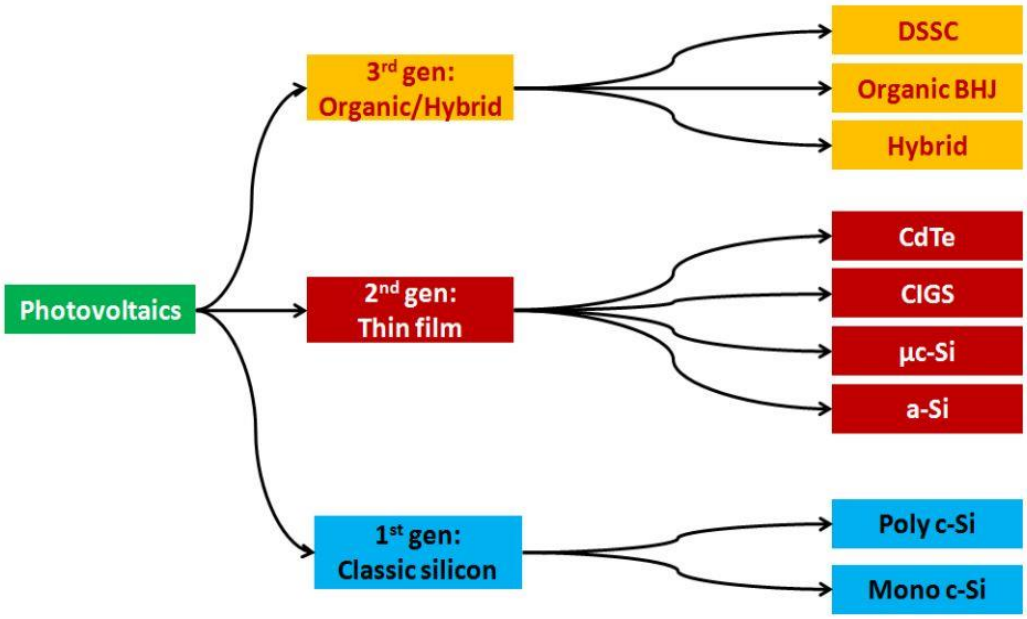

Figure 1-3 Development of Different Generations of Solar PV

1.2.1 Solar cells Generations

Depending on the type of formed junction, manufacturing technique used, and photon absorbing material type, photovoltaics are divided into three main generations.

1. Wafer-based crystalline silicon bulk multi-junction solar cell (‘First Generation Solar Cells’)
2. Thin film solar cells Amorphous Silicon (a-Si), Copper-Indium-Gallium-Diselenide solar cells (CIGS), Cadmium Telluride solar cells (CdTe), etc (‘Second Generation Solar Cells’)
3. Emerging Technologies (polymer-based organic solar cells, Dye Sensitized solar cells(DSSCs), Perovskite cells) etc. (‘Third Generation Solar Cells’)

1.2.1.1 Wafer-based Crystalline Solar Cells

Most of the solar panels are fabricated using this technology which is further classified into two categories.

1.2.1.1.1 Monocrystalline Solar Cells

The most common, established, reliable, and developed of all solar cells are monocrystalline cells which are 18-20% efficient. Using a process called the Czochralski process [22], a single crystal of silicons is used to make solar cells. During manufacturing, silicon crystals are cut from the cylindrical ingots and used in forming a single cell. Later, multiple units are joined forming a module. The theoretical efficiency of these cells is considered to be around ~30% which is quite high[23]. In addition to high efficiency, the cells have a longer life, more electricity production, and high heat resistance. On the other hand, these modules have a disadvantage in terms of the initial cost. Since a costly and complex manufacturing process is applied in forming these cells.

1.2.1.1.2 Polycrystalline Solar Cells

Polycrystalline solar cells is the second category among first generation solar cells. As the name indicates, the solar cell wafer used in manufacturing these cells is cut from an ingot of a multifaceted polycrystalline silicon. As a result, the uniformity and alignment obtained are not comparable with that of monocrystalline solar cells. Furthermore, there are losses at the joints between them which leads to lower efficiency. On the other hand, under certain circumstances, this grain misalignment can help as light is hitting from all angles. An example would be good working in low light in comparison with monocrystalline solar cells. On of the main advantages of polycrystalline solar cells is their cost-effectiveness. Further, these cells are also easy to

produce. As far as manufacturing is concerned, these cells are produced by cooling a graphite mold containing molten silicon. Afterwards, this molten silicon is transferred into blocks sawed in the plates. The next phase is solidification during which, crystal structures of different sizes are formed. Module level efficiency r cells. With the benefit of low initial cost, the low efficiency is the undesirable trait [24].of these cells is around 12-14% which is quite low as compared to monocrystalline solar cells.

1.2.1.2 Thin Film Solar Cells

Thin film solar cells have stacked thin layers, usually one or more, of photovoltaic materials which are deposited upon the substrate. It's thickness can vary in the range of nanometers to micrometers. Different cells are manufactured by depositing photovoltaic materials using a variety of deposition techniques on a range of substrates. The photovoltaic material used to make thin-film solar cells is typically used to categorise them [25]. In thin film solar cells, amorphouse silicon solar cells, cadmium telluride solar cells, and copper-indium-gallium-selenide(CIGS)solar cells are famous.

1.2.1.3 Organic and Hybrid Solar cells

Organic solar cells are polymer based cells which use organic polymers for the photovoltaic effect. On comparison with silicon solar cells, organic cells are light weighted, cheap, flexible, and recycleable. Further, organic solar cells are environmental friendly. As far as disadvantages are concerned, they have a low efficiency and hence most of the solar cells are inorganic [26]. Maximum achieved efficiency of organic solar cells is almost 9% [27]. Hybrid solar cells employ both organic as well as inorganic materials in which organic elements are used for absorption of light whereas electron transport material is mainly inorganic in nature. Efficiency of these cells is dependent upon effective manufacturing of interface between organic and inorganic materials are made [28]. Hybrid solar cells include dye sensitized solar cells (DSSCs) and polymer nanocompoiste solar cells.

1.2.1.3.1 Dye-Sensitized Solar Cells (DSSCs)

In 1991, Gratzel and O'Reagan discovered DSSCs which are third generation solar cells working on principle of photosynthesis. These cells contain a moleculer dye which absorbs light from sun in the same way cholorophyll does in plant leaves. This molecular dye is pasted upon a layer of titanium dioxide nanoparticles and this thin layer is porous in nature. Titanium Dioxide is immersd in an electrolyte solution. To complete the cell, platinum is used as a counter-electrode.

Assembling these cells in this chemical way makes them more facile and cost effective [29]. Ruthemium based organic dyes especially N719 are used as sensitizers in the DSSCs cells. The photoanode has a thick film of transparent titanium dioxide nanoparticles that scatter photons back into the transparent film whereas platinum is used as the counter electrode.

1.3 Working of a solar cell

When solar cell is placed in the ambient environment in the presence of sunlight, then photon of sunlight (energy packets) gives energy to the solar cell to produce an electric current. Overall solar cell working comprises of three main steps,

- Absorption of sunlight
- Charge separation
- Conduction or charge collection

First solar light is absorbed in the visible range of 400nm-700nm wavelength by the surface of a solar cell, which comes through the glass. Cell absorbs the visible spectra and the energy required to break the depletion region is provided to get the enough energy to go from valence band to conduction band. In that way, all the holes and electrons goes towards their sides, holes moves towards p side while electrons moves towards the n side, charges are separated. Now, solar cell has develop potential difference and if it connected to a load, it enlightens the load and in that conduction takes place. Electrons going from the n-type layers through the external circuit goes to the p-side region, where electrons meet with the holes and this cycle of conduction continues until the enough energy photons are being received by the solar cells to break the junction barrier.

1.4 Problem Statement

Development of photovltaics technologies with high efficiency and affordablility has always been an esteemed area of interest for the material scientists and device community. Dye-sensitized solar cells are a potential technology for renewable energy development due to their short energy recovery time, ease of assembly, and excellent ability to achieve eco-friendly properties. In order to complete the process of converting light into electricity, the counter electrode in DSSCs must both deliver the electron and catalyse the regeneration of iodide from

triiodide. Due to its high electrical conductivity and exceptional catalytic capacity to regenerate iodide from triiodide, platinum (Pt) is the most often utilised material for counter electrodes. The investigations utilising Pt counter electrodes yielded many important conclusions that served as the cornerstone of DSSC technology. The noble and precious nature of Pt, as well as its poor stability in the electrolyte, have, nevertheless, been a key barrier to realising low-cost, and therefore large-scale deployment of DSSCs with the goal of extending solar power up to the terawatt scale. Among them carbon based materials especially derived from biomass have the earmark of being used as counter electrode as they tend to possess the properties like large surface area, excellent corrosion resistance, more conductivity, ability to catalyzed the redox reactions plus the cost effectiveness and readily availability. Along with a number of benefits, hemp (cannabis) has a tremendous deal of potential for renewable energy. In addition to growing largely in all types of habitats and temperatures, it is also more environmentally friendly. It has a high dry matter yield, low cost, mild nutrient requirements for growth, low pesticide requirement, and a high biomass content. In this study, Hemp has been used as precursor to prepare activated carbon with high porosity and large surface area which then was used to fabricate the counter electrode to replace the conventional platinum counter electrodes.

1.5 Objectives

Future solar cells using Dye sensitization technology are ever developing and auspicious field of study with lots of potential to evolve over time. The anticipated objectives of current research work pertain to development of DSSC's cells are as follow:

- To synthesize the activated carbon derived from hemp based biomass through green synthesis process
- To characterize the prepared hemp based carbon via certain characterization techniques
- To fabricate the counter electrode using hemp activated carbon
- To study the structural, morphological as well as the electrochemical properties of the fabricated counter electrodes
- To establish the comparative analysis of hemp activated carbon with the conventional (commercial) activated carbon and platinum based countr electrodes.

1.6 Limitations

The following limitations prove to be hurdle in order toevaluatethefull potentionalof hemp activated carbon as suitable candidate for counter electrode fabrication of DSSCs. By overcoming theses challenges the foundations can be led to level up the solar industry to combat the current energy crisis as well as to commercialize the Dye sensitized solar cells.

- Pohotovoltaic characteristics of hemp based counter electrodes can not be determined as the I-V curves was not recorded due to unavailability of said facility.
- Relaiability and stability issues.

1.7 Thesis outline

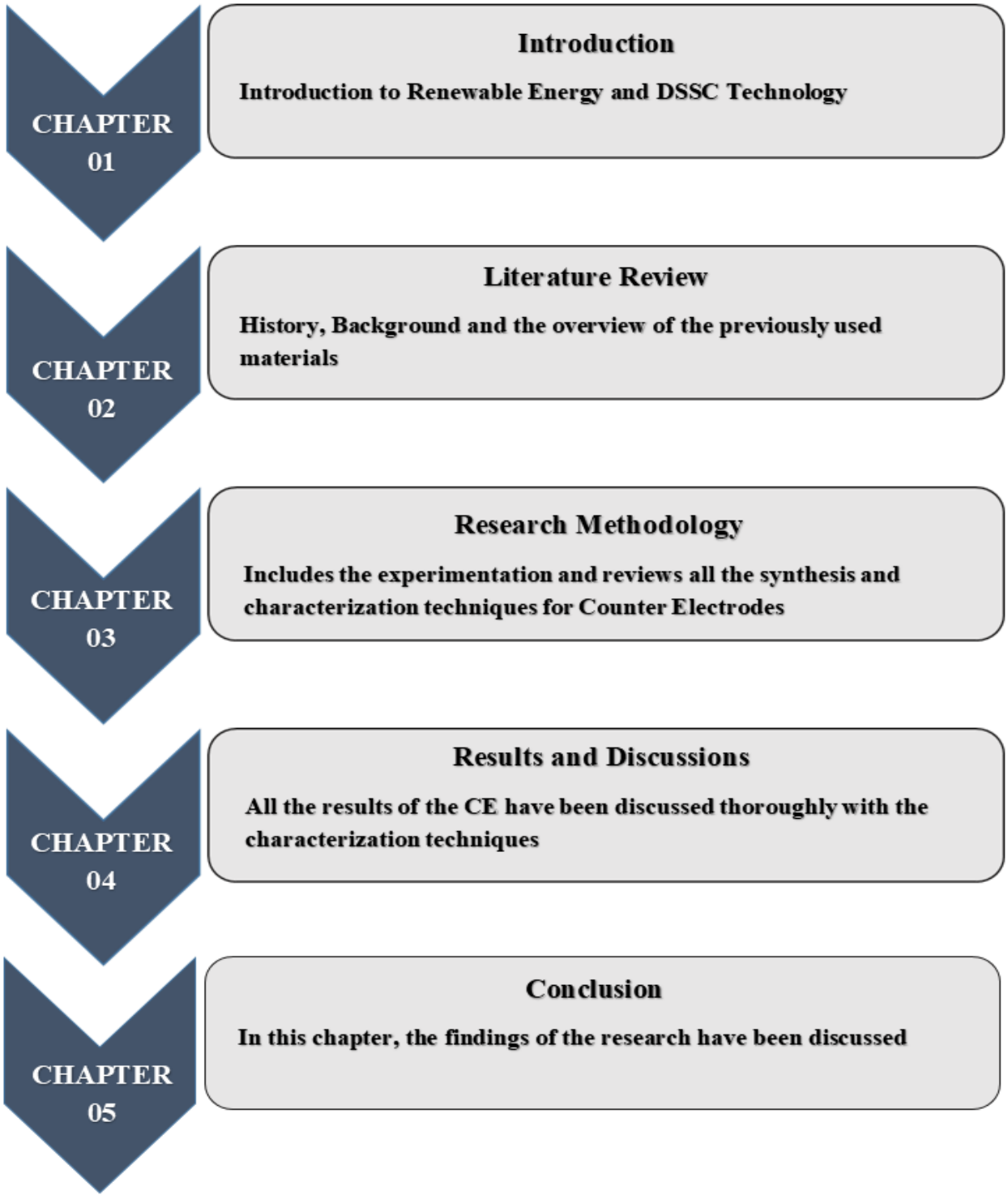

Figure 1-4 Figure Depicting Flow of Thesis

1.8 Scope of thesis

Dye sensitised solar cells (DSSC) are a type of solar cell that is gaining popularity among scientists and researchers. The substitution of activated carbon for platinum-based counter electrodes can reduce the cost of various energy storage and conversion processes. The synthesis of activated carbon from biomass is of current interest in terms of energy sustainability. The carbonization process has a significant impact on the properties of activated carbon derived from biomass. This research focuses on the chemical activation of hemp to produce activated carbon with a very large surface area and high porosity. The hemp leaves were first carbonised at 750°C before being activated with hydrogen peroxide (H2O2). Doctor Blade coating Technique was then used to create a carbonaceous counter electrode containing Hemp activated carbon (HAC) on an FTO glass substrate. The photoanode was prepared, and the DSSC was finally assembled. Various characterization techniques were used, including XRD, FTIR, SEM, Raman Spectroscopy, and Cyclic Voltammetry. SEM was used to examine the surface morphology, which revealed the development of a regular porous structure. FTIR confirmed surface functional groups such as -OH, -COOH, and -C=C/C-C. Raman spectroscopy and X-ray diffraction were used to determine the crystalline and graphite nature of HAC. This study proposes an environmentally friendly method for mass-producing activated carbon from hemp.

1.9 Summary

The concept of solar energy, photovoltaic technology, and other related terminologies in the solar cell are explained in detail. All the generations of solar cells were also described with their characteristics and a special focus on the cell, dye-sensitized solar cell with their basic principle of working, components, and their applications, as well as the features that give this generation edge over the other generation of solar cells.

1.10 References

[1] "Knowledge, perception and awareness of renewable energy by engineering students in Nigeria: A need for the undergraduate engineering program adjustment | Elsevier Enhanced Reader."

[2] A. Harjanne and J. M. Korhonen, "Abandoning the concept of renewable energy," *Energy Policy*, vol. 127, no. December 2018, pp. 330–340, 2019.

[3] H. Lund, "Renewable energy strategies for sustainable development," *Energy*, vol. 32, pp. 912–919, 2007.

[4] W. Wang, L. W. Fan, and P. Zhou, "Evolution of global fossil fuel trade dependencies," *Energy*, vol. 238, p. 121924, 2022.

[5] H. van Asselt, "Governing fossil fuel production in the age of climate disruption: Towards an international law of 'leaving it in the ground,'" *Earth Syst. Gov.*, vol. 9, p. 100118, 2021.

[6] R. E. N. Members, *Renewables 2021 global status report 2021*. 2021.

[7] "When Fossil Fuels Run Out, What Then? - MAHB." [Online]. Available: https://mahb.stanford.edu/library-item/fossil-fuels-run/. [Accessed: 11-Jan-2022].

[8] I. Energy Agency, "Renewables 2021 - Analysis and forecast to 2026," 2021.

[9] "Solar energy potential assessment: A framework to integrate geographic, technological, and economic indices for a potential analysis | Elsevier Enhanced Reader."

[10] "Solar Photovoltaic Power Potential by Country." [Online]. Available: https://www.worldbank.org/en/topic/energy/publication/solar-photovoltaic-power-potential-by-country. [Accessed: 11-Jan-2022].

[11] "The linkage between renewable energy potential and sustainable development: Understanding solar energy variability and photovoltaic power potential in Tibet, China | Elsevier Enhanced Reader."

[12] "Passive Solar History." [Online]. Available: http://californiasolarcenter.org/old-pages-

with-inbound-links/history-pv/. [Accessed: 13-Jan-2022].

[13] M. Taguchi, A. Suzuki, N. Ueoka, and T. Oku, “The History of Solar,” *AIP Conf. Proc.*, vol. 2067, 2019.

[14] “Solar Photovoltaic Technology Basics | NREL.” [Online]. Available: https://www.nrel.gov/research/re-photovoltaics.html. [Accessed: 13-Jan-2022].

[15] “How a Solar Cell Works - American Chemical Society.”

[16] “(20) (PDF) Temperature Effect on Power Drop of Different Photovoltaic Modules.”

[17] “Method to determine the single curve IV characteristic parameter of solar cell.”

[18] S. Ananthakumar, J. R. Kumar, and S. M. Babu, “Third-Generation Solar Cells: Concept, Materials and Performance - An Overview,” pp. 305–339, 2019.

[19] K. Sharma, V. Sharma, and S. S. Sharma, “Dye-Sensitized Solar Cells: Fundamentals and Current Status.”

[20] Y.-H. Fan, C.-Y. Ho, and Y.-J. Chang, “Enhancement of Dye-Sensitized Solar Cells Efficiency Using Mixed-Phase TiO 2 Nanoparticles as Photoanode,” 2017.

[21] Mitch Jacoby, “Commercializing low-cost solar cells,” *C&EN Glob. Enterp.*, vol. 94, no. 18, pp. 30–35, May 2016.

[22] F. Yu, Y. Shi, W. Yao, S. Han, and J. Ma, “A new breakthrough for graphene/carbon nanotubes as CEs of dye-sensitized solar cells with up to a 10.69% power conversion efficiency,” *J. Power Sources*, vol. 412, no. October 2018, pp. 366–373, 2019.

[23] S. A. Almohsin, M. Mohammed, Z. Li, M. A. Thomas, K. Y. Wu, and J. B. Cui, “Multi-walled carbon nanotubes as a new CE for dye-sensitized solar cells,” *J. Nanosci. Nanotechnol.*, vol. 12, no. 3, pp. 2374–2379, 2012.

[24] “Synergetic Effects of Hybrid Carbon NanostructuredCEs for Dye.pdf.” .

[25] S. Farooq, A. A. Tahir, U. Krewer, A. ul H. A. Shah, and S. Bilal, “Efficient photocatalysis through conductive polymer coated FTO CE in platinum free dye sensitized solar cells,” *Electrochim. Acta*, vol. 320, p. 134544, 2019.

[26] C. Wu, G. Li, X. Cao, B. Lei, and X. Gao, “Carbon nitride transparent CE prepared by magnetron sputtering for a dye-sensitized solar cell,” *Green Energy Environ.*, vol. 2, no. 3, pp. 302–309, 2017.

[27] S. Prasad *et al.*, “3D nanorhombus nickel nitride as stable and cost-effective CEs for dye-sensitized solar cells and supercapacitor applications,” *RSC Adv.*, vol. 8, no. 16, pp. 8828–8835, 2018.

[28] U. Ahmed, M. Alizadeh, N. Abd, S. Shahabuddin, M. Shakeel, and A. K. Pandey, “A comprehensive review on CEs for dye sensitized solar cells : A special focus on Pt-TCO free CEs,” *Sol. Energy*, vol. 174, no. October, pp. 1097–1125, 2018.

[29] Ş. Sungur, “Titanium Dioxide Nanoparticles,” *Handb. Nanomater. Nanocomposites Energy Environ. Appl.*, pp. 713–730, 2021.

Chapter 2: Literature Review

With the increasing energy demand, renewable energies are presenting an alternative especially solar renewable energy is growing day by day for the countries situated in the rich solar region. Among the various solar cell products available in the market Dye-Sensitized Solar Cells (DSSC) are the latest one. These Solar Cells mimics the natural processes of photosynthesis and appear to be cheaper than conventional solar cells and offer ease of processing (fabrication) from the rest of the photovoltaics.

2.1 History and Origin of Solar Cells

The interaction of humans with technology involving solar energy dates back to the 7th century [1] when sunlight was used to set fires and burn ants by focusing it on glass and mirrors [2]. But today solar energy has been advanced into very innovative technologies e.g., solar-powered vehicles and airplanes.

Romans and Greeks, the superpowers from the 3rd century used to focus sunlight to lit the torches whereas the Chinese practiced the same in 20th AD [3]. In the 4th century AD, the water in Roman bathhouses was warmed through large windows facing south to let the rays of the sun come in. In the 1830s, Sir Johan Herschel used the world's first solar collector for cooking during his expedition to South Africa. This solar collector was built by Horace de Saussure [4]. Robert Stirling, on September 27, 1816, was the first person who applied for a patent in Edinburgh, Scotland as he developed a heat engine **"eEonomizer"** that was used to produce power through the sun's thermal energy, in a solar thermal electric technology [5-7].

Until 1839 the photovoltaic effect was not known to the world, when a French scientist, Edmond Becquerel discovered it during his work with an electrolytic cell [8]. Two metal rods immersed in a solution (able to conduct electricity) constituted this electrolytic cell and showed significant improvement in the generation of electricity when they were exposed to sunlight. A French mathematician Auguste Mouchaet along with his assistance built the precursor of the modern-day parabolic solar dish collector, a solar-powered engine used in the 1860s for enormous applications [9]. The photoconductivity of selenium was discovered by Willoughby Smith and Williams Gryells along with Richard Evans in 1873 and 1876 respectively. A paper with the title "The action of light on selenium" was also published by these researchers. Similarly, in 1883,

Charles Fritts was the first person who fabricated a solar cell based on wafers of selenium. In 1887, Heinrich Hertz discovered that the lowest voltage that can cause a spark to jump between two metal electrodes can be altered by ultraviolet light. Wilhelm Hallwachs in 1904, discovered that cuprous oxide, as well as copper, are photosensitive, and he made a semiconductor junction solar cell using these oxides. Based on the publication of Albert Einstein explaining the photoelectric effect per quantum mechanics, 10 years later, the existence of a barrier layer in photo voltaic (PV) devices, finally, was explored. In 1916, Roberts Milikan experimentally proved the photoelectric effect. Single-crystal silicon growing method was discovered by Jan Czochralski. A material that is still used by the PV industry is cadmium selenide, its photovoltaic effect was discovered by Audobert and Stora in the year 1932. The method of crystal growth that was developed by Czochralski was adopted by Gordon Teal with John Little, in 1948, for the production of single crystal germanium and then later for silicon [10]. Bell Laboratories on April 25, 1954, announced their first ever practical silicon based solar cell having an efficiency of 6% [11-12]. In 1955, Western Electric got a license for solar cell-based technology, during the same period, the Semiconductor Division of Hoffman Electronics Semiconductor Division came out with commercial solar cell technologies that were 2% efficient, later on, 9% efficient solar cell was also created by them. In 1958, Mandelkorn T of U.S. Signals Corps Laboratories fashioned an n-upon-p silicon-based solar cell. The damage caused by ultraviolet radiation was lesser on these cells and thus was best suited to be used in space. Vanguard 1, a solar-based satellite, the first of its kind was powered with 0.1 watts, 100 cm^2 solar panels. Later on, the first Photovoltaic cell with amorphous silicon, having an efficiency of 1.1% was fabricated by Wronski and Carlson at R.C.A. Laboratories in 1976. In 1980, at Delaware University, The Institute of Energy Conversion (IEC) designed a thin film-based solar energy cell using Copper Sulfide and Cadmium Sulfide (Cu_2S/CdS) showing efficiency of approx. 10%. The Centre for Photovoltaic Engineering (CPE) at the New South Wales University (UNSW) achieved 20% efficiency for silicon cells. Bryan O'Reagan and Micheal Gratzel created DSSC in 1988. The cost of these photo-electro-chemical solar cells was almost half of the silicon solar cells and their operation was based on an organic dye compound.

As far as the history of solar cell technology is concerned, a breakthrough and a new world record were achieved in 2006 that the efficiency of solar cells came up to 40%, thus breaking the sunlight to electricity barrier [13]. The scientists at National Renewable Energy Laboratory

(NREL) break this record by fabricating a PV device that showed a high conversion rate for the incident light and turning it into electricity. The efficiency of this device was 40.8%. However, this was achieved only under concentrated energy then an inverted solar cell was constructed with a metamorphic triple-junction and autonomously measured precisely at NREL [14]. Later in 2011, the Chinese companies pushed down the manufacturing costs for silicon-based PV modules to about $1.25 per watt. Consequently, the installation of solar cells doubled worldwide. Research and development on Photovoltaic devices continue with a more intense focus on raw materials, novel approaches, and cell design towards solar favoured materials and products manufacturing [15].

2.2 Development of the Solar Cells

The terminology Photovoltaic has found its origin in Greek words “Photo” meaning light and voltaics which means electricity after the name of Alhessandro Volta, the physicist who designed the electric battery. Photovoltaics usually refers to the alteration of solar energy which is light energy to electricity. However, associated physical phenomenon of photovoltaic effect was first understood by Alexandro Edmand Bacquerel while working with metallic electrodes and electrolytes. In 1833, the first solar cells made up of selenium wafers were designed, by Charles Fritts who was an American inventor and in 1888, the first US patent for solar cell was earned by Edwerd Weaston. In 1901, An American patent titled “method of utilizing and apparatus for the utilization of radiant energy” was received by Nikola Tesla [16]. Published in 1905, the paper published by Einstien proposed the theoretical background for the photoelectric effect [17]. The experimental proof for Einstein’s theory of photoelectric effect was provided by Robert Millikan in 1916. After this success, in 1922, Einstein received Physics Nobel Prize for his work on the photoelectric effect. Around 30 years later, at Bell labs, the team developed Si-based solar cells after discovering the photoelectric effect exhibited by Silicon and achieved 6% efficiency. These first solar cells found their applications in early satellites. Initially, the advancements in the field of solar technology were concentrated on space-related applications.

However, after the oil shock (oil crisis) of 1970, alternative energy sources gained real importance when in mere time span of six months. the oil prices doubled. The issues related to ever-growing concerns such as global warming and following climate change encouraged the use of renewable resources. In order to overcome both the environmental issues and energy crisis,

the world leaders decided to reduce the emissions of greenhouse gases (mainly CO_2), in Kyoto Protocol, the goal was to reduce emissions by at least 5.2% in 2012 as compared to the levels which were recorded in 1990. As a result, a conducive environment for the exponential growth of renewable energy resources was created mainly photovoltaic industry. Nowadays, photovoltaic industry is among the leading industry based on renewable energy resources [18].

2.3 Emergence of Dye-Sensitized Solar Cells

Amongst already existing solar cells, the Dye-Sensitized Solar cells (DSSC) are the new ones that basically mimics the natural process of photosynthesis. DSSC are gaining importance because of their less costs and requires less expertise for fabrication than conventional solar cells. Fundamental concept of DSSC is based upon the photoelectric experiments conducted by Becquerel in 1839 in which platinum-based electrodes were dipped in an electrolyte which contained the halide (metal) salt to produce current. To encompass the photosensitivity of silver halide, a dye was added to absorb at longer wavelength, this discovery was made by Vogel in 1883 [19]. In 1887, Moser surprised the chemists by the introducing the concept of a dye on the silver halide electrodes for the photo-electro-chemical cells [20]. In 1964, Namba and Hishki recognized the effectiveness of cyanine and combining two cyanine dyes to have a photochemical process [21]. Later on, the addition of dye on the semiconductor electrodes became a common consensus to enhance efficiency of photo-electro-chemical cells. The base of modern photo electrochemistry was led by Brattain and Garret. The study on semiconductor-electrolyte interface was first time studied by Gerischer in photoelectrochemical cells [22,23]. A worldwide quest for alternative energy sources was set in 1973 after the oil crisis with large studies aimed at photo-electro-chemical cells. However, the sensitization of a photo electrode was first performed in 1870s according to Gratzel. The understanding of the two procedures did not occur until 1960s, that both the procedures worked similarly, by injection of the electrons from photoexcited dye molecules into the conduction band of the n-type semiconductor. Afterwards, in succeeding years, to increase the efficiency of dye, it was suggested that it should be absorbed chemically on the outer surface of relative semiconductor. Dispersed particles provide sufficient interface when employed to photo-electrodes [24].

Owing to its biocompatibility, readily availability, less cost and nontoxicity titanium dioxide became the semiconductor of prime importance and used for sensitized photo-electrochemistry.

Whereas, tris (2,2 bipyridyl-4, 4 carboxylate) Ruthenium (II) was the dye utilized as standard. In 1991, after extensive research, sensitized electro-chemical photovoltaic devices with the conversion efficiency of approximately 7.2% upon irradiation by sunlight, were formed. Progressively the evolution of further competent DSSC has continued with conversion efficiency over 10%.

2.4 Operating principle of Dye-Sensitized Solar Cells

Under illumination, DSSCs are designed to use the photo-electrochemical mechanism in order to convert light energy to useable energy [25]. Unlike solar cells based on p-n junctions, DSSCs are designed to operate similar to photosynthesis process operating in plants thus allowing for individual customization of absorption of light and charge transfer process, allowing far wider material design freedom. Because of their exceptional capacity to achieve a quick energy-payback, easy manufacturing and environment friendly qualities, DSSCs are quite a reliable addition in renewable energy field.

A glance at Fig. 2.1 shows that a simple DSSC setup has two electrodes: a photoanode i.e. working electrode and a photocathode i.e. the counter electrode. By coating a dye loaded porous Titanium Oxide ($TiO_{2)}$ nanoparticle film on a transparent conducting oxide (TCO), the working electrode is made. On the other hand, the counter-electrode is platinum NP coated transparent conducting oxide (TCO). A liquid electrolyte (a redox pair) is put between these two electrodes. When light strikes the photoanode travelling through TCO, dye molecules are activated and transfer an electron to TiO_2's conduction band (CB) since dye's HOMO is higher than TiO_2's CB. Diffusion allows the transferred electron to reach the TCO through the TiO_2 nanoparticle layer.

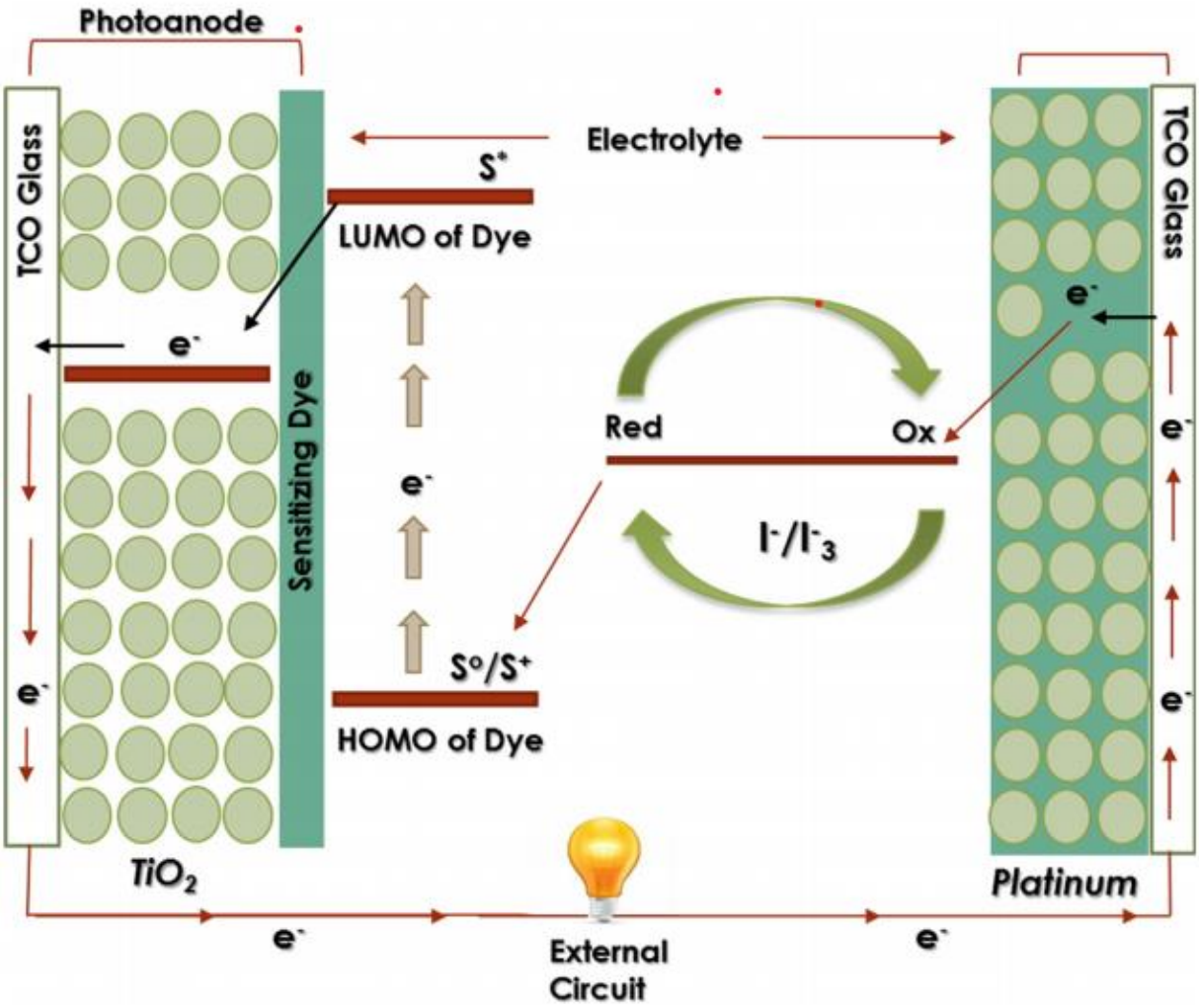

Figure 2-1 Schematic diagram and basic working principle of DSSC

On the other hand, the oxidized dye molecule is regenerated by taking an electron from the redox pair in the form of iodine/triiodide species. Furthermore, an electron can also be absorbed from external circuit's counter electrode to recreate this redox pair. The following steps are involved in electron transfer during cell operation [26,27]

a) **Photo absorption and dye excitation:** In the very first step excitation of dye takes place upon irradiation with solar light and promoted to excited state from ground state according to following equation:

$$TiO_2|S + hv \rightarrow TiO_2|S^* \quad \text{..... Eq 2.1}$$

b) **Electron injection:** The excited dye oxidized and injects electron into the conduction band of the semiconductor film. The rate at which this process occurs is 1010 to 1012s-1.

$$TiO_2|S^* \rightarrow TiO_2|S^+ + e^- \quad \text{..... Eq 2.2}$$

c) **Recovery of dye:** In this step dye recovers its original state i.e., de-excited to ground state as:

$$TiO_2|S^+ + e^- \rightarrow TiO_2|S \quad \text{..... Eq 2.3}$$

d) **Oxidation of electrolyte:** Oxidization of electrolyte takes place according to following equation:

$$TiO_2|S^+ + \frac{3}{2}I^- \rightarrow TiO_2 + \frac{1}{2}I_3^- \quad \text{..... Eq 2.4}$$

e) Regeneration of electrolyte:

The restoration of electrolyte happens at the counter.

$$\frac{1}{2}I_3^- + e^- \rightarrow \frac{3}{2}I^- \quad \text{..... Eq 2.5}$$

f) Oxidation -reduction reaction

$$I_3^- + 2e^- \rightarrow 3I^- \quad \text{..... Eq 2.6}$$

Whereas,

S represents dye sensitizer, S* represents excitation phase, S+ represents oxidized dye

In order to enhance light transmission and electrical conductivity, a conductive glass is used as the substrate. This glass is divided into fluorine-doped tin oxide (FTO) and indium-doped tin oxide (ITO). A thin film of TiO2 nanoparticles is used as semiconductor electrode placed over a glass film having a thickness around 11-16 micrometers. This electrode plays a significant part in the separation of exciton and transfer of electron. The amount of dye molecules absorbed on the TiO2 layer's surface is mostly determined by its porosity and shape.

2.5 Components of DSSCS and their properties

DSSCs are composed of five components;

1. Transparent Conducting Substrate (TCO)
2. A metal oxide coating
3. Dye

4. An electrolyte
5. Counter-electrode material

2.5.1 Transparent conducting substrate

The DSSC's performance is heavily influenced by the clear conducting substrate. In DSSC, it serves two functions: (1) current collector, (2) a support for the semiconductor layer. TCO has two key characteristics: firstly, greatly transparent thus allowing more light that can pass to the underside of active material and secondly, low electrical resistivity that in turns, speed up the transfer of electron. Among transparent conducting oxides used in industry, majority are conductors of n-type.

Both inorganic and organic materials have been used to create transparent conducting coatings for solar purposes. A layer of TCO [28], such as FTO (Fluorine doped Tin Oxide), ITO (Indium Tin Oxide) and Zinc Oxide (doped) is commonly used in inorganic films. To create organic films, grapheme and nanotube networks of carbon are being used. Transparent glass coated with FTO/ITO substrates are most efficient TCO materials extensively utilized in solar applications. However, the main shortcoming of ITO is, its conductivity degrades with time. In the manufacturing of DSSCs, the calcinations method is used. As a result, FTO is the transparent option of choice. For DSSCs, there is a conducting substance. Deposition of TCO films is done on the substrate by a variety of methods. Spray pyrolysis, Pulsed Laser (PL) Deposition and Metal Organic Vapor Deposition (MOCVD) are some of deposition processes used, although magnetron deposition is the most effective. The film is sputtering [29].

2.5.2 Semiconductor Photoanode: metal oxide coating

The photoanode is a critical component of the DSSC, as it is involved in (a) dye loading, (b) electron injection, (c) transportation, and (d) collection. As a result, it has a major impact on current, voltage, and efficiency of power conversion. Material structures of different types have been created including Zero Dimensional (0D), One Dimensional (1D) also known as Quasi Dimensional, and hierarchal nanostructures. The final arrangement, in particular, has a lot of potential for producing high-performance DSSCs.

As a result, the photoanode materials must fulfil a number of requirements: First, to guarantee an efficient movement of electrons (photo-induced) from dyes to the subsequent semiconductor layer, the conduction band edge of semiconductor should lie below the lowest unoccupied

molecular orbital (LUMO) of the dye molecules. Second, the surface area of semiconductor film should be large so more dye molecules are absorbed. Third, the porosity of semiconductor film should be high enough so that the electrolyte infiltrates deeply inside film thus giving better Ohmic contact across the interfaces. Fourth, to easily move electrons to outer circuit, the electron mobility of semiconductor should be high. Different n-type oxides, such as Titanium Oxide (TiO_2) [30] Zinc Oxide (ZnO), [31-32] Stannic Oxide (SnO2) [31-34], and other ternary oxides, such as Zn_2SnO_4 [35], can be used as metal oxides. However, TiO_2 is most commonly used since it effectively meets the above-mentioned requirements. As a result, it is also known as the DSSC's "workhorse," "vehicle," or "heart."

The photoanode's shape was also employed to increase light scattering and electron transport. Nanotubes, large particles, nanospindles, nanowires, nano-embossed hollow spheres, electrospun fibers, and other forms of crystals, hexagonal plates, and hexagonal plates have all been studied [36]. A bilayer structure made up of a scattering layer and a nanosized transparent layer has recently received a lot of interest due to its ability to improve device performance by efficiently increasing light scattering. Double light-scattering films [37], surface plasmon effects [38-40], 1-3D nanostructured designs [41], quintuple-shelled hollow microspheres [42], and multi-stack structures are all explored as scattering layer structural designs [43].

2.5.3 The Sensitizer

In the DSSC, the dye monolayer is a key component for converting incident light into electricity. When exposed to sunlight, dyes' molecules undergo an electrical shift from the initial ground state to the energy laden excited state. An ultrafast electron injection from the excited state of dye molecule to the conduction band of titanium oxide (TiO2) allows the electron to be transported out through TiO_2. Several criteria must be met by the ideal sensitizer in order for molecular engineering to be effective: (a) The sensitizer must have the ability to absorb light over a wide range of wavelength spectrum, up to infrared; (b) it must anchor on the surface of semiconductor oxide by means of a phosphine or carboxylate group ; (c) to avoid potential energy loss during the process of electronic transfer, LUMO of the sensitizer should be above the edge of the conduction band of oxide, (d) The highest occupied orbital (HOMO) of sensitizer must be low for easy electron or hole transfer; (d) the sensitizer must be of stable nature. Typically, the metal oxide nanoparticles are immersed in the dye containing solution for a period

of 12-24 hours resulting in adsorption of dye molecules on the surface of nanoparticles of metal oxide.

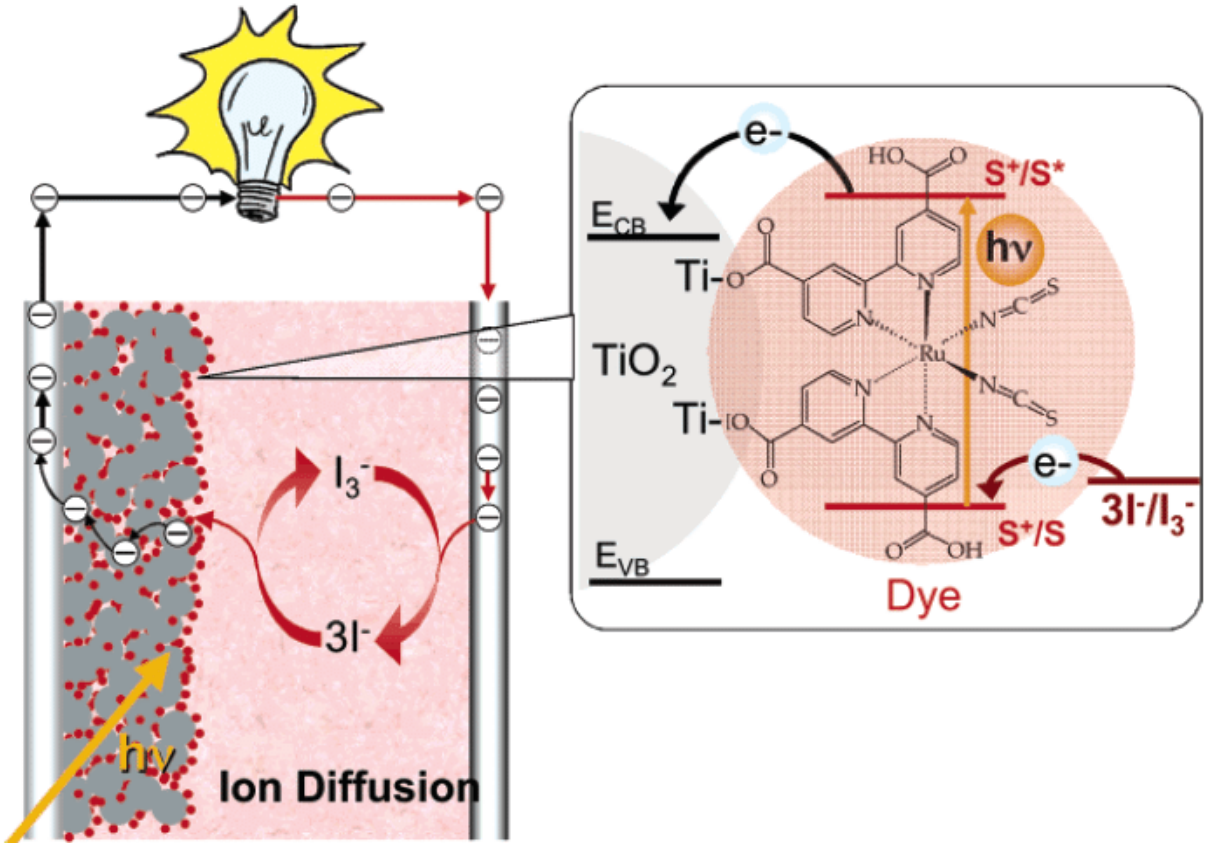

Figure 2-2 Conversion of incident light to electricity with dye molecules

Considering upto wavelength of 750nm, Rutheniser 535-TBA (N 719) and Rutheniser 535 (N 3) dyes are amongst most effective sensitizers in dye solar cells. However, when considering the entire range of absorption, black dye outperforms in terms of performance. But researchers are looking for metal free organic dyes because of cost, availability and restricted quantity of noble metals. Complex manufacturing and purification further adds to the search of metal free dyes [44]

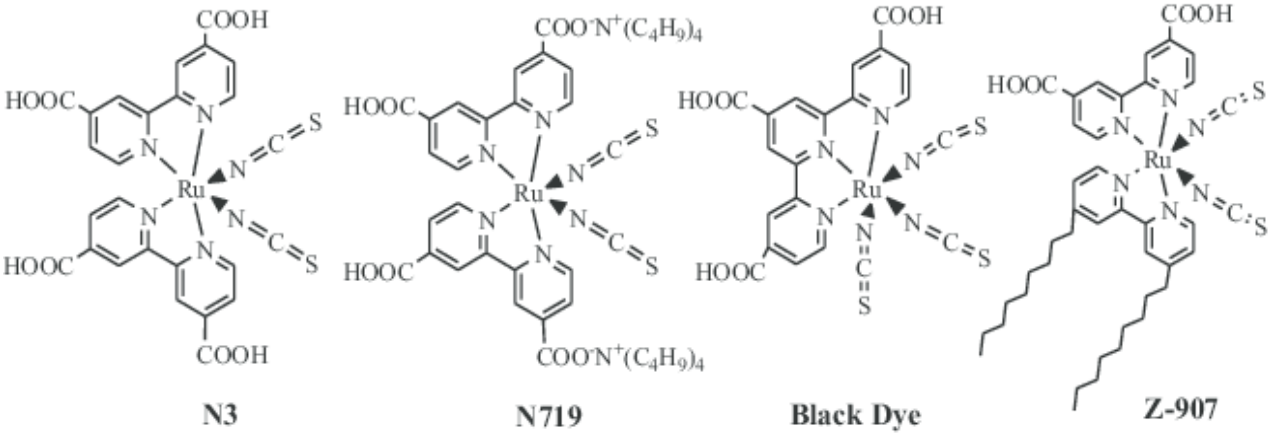

Figure 2-3 Conversion of incident light to electricity with dye molecules

Metal-free dyes have lately received a lot of interest due to their greater molecular design flexibility and better molar extinction coefficients. Due to the versatility of structural design, a donor-pi-acceptor (D-π-A) structure integrated dye has recently emerged as a potential method to enhance dye properties [45, 46]. Many researches have been conducted to enhance the characteristics of D-π-A dyes like absorbance, longer stability, rate of charge recombination, and efficiency of injection by adjusting the different donor groups, designing conjugated bridge, and optimization of acceptors or anchors [47]. Yella and coworkers [48] created a dye named donor-p-bridge-acceptor zinc porphyrin (YD2-O-C8). It inhibits, across faces, electron back transfer from the TiO2 layer to oxidized mediator i.e. cobalt. This in turns results into 12.3% power conversion efficiency when put under simulated air mass of 1.5 global sunshine.

2.5.4 The Electrolyte

The electrolyte is needed for absorption of electrons at cathode and transfer them to the oxidized molecules of dye thus regeneration of electrons. Iodide (I-) or TriIodide (I3-) are among the widely used electrolytes because they have performed effectively to their kinetics and suitable energy levels [49]. The redox potential of an ideal electrolyte should be higher than the dye's LUMO. I3- diffuses to the cathode in the electrolyte to capture electrons, then generates I-, so to renew dye molecules, I- diffuses in opposite way to the electrode (TiO2). As a result, electrolyte's diffusion characteristics should be sufficient to prevent mass-transport restrictions. It also has to be non-corrosive to metal collectors and have high photochemical stability.

The difference between electrolyte's redox potential and quasi Fermi level of Titanium Oxide (TiO2), which is around 0.6 – 0.7 V under the solar illumination circumstances, determines the highest voltage produced in DSSCs in theory. On the other hand, different redox couples like Br^- or Br^{3-}, SCN^- or $(SCN)^2$, $SeCN^-$ or $(SeCN)^{3-}$, $Fe(CN)_6^{3-}$ or $Fe(CN)_6^{4-}$ [50], and Co(II) or Co(III) complex have also been added in DSSCs for production of a large open circuit voltage and also, to limit corrosion of the I^- or I^{3-} redox couples.

2.5.5 Counter electrode

Platinum nanoparticles are typically the counter electrode coated on fluorine-doped tin oxide (FTO) in DSSCs. In I- / I3- redox regeneration, the I3- to I- conversion is very effective on surface of platinum (Pt) counter electrode which helps in oxidized dye regeneration. Thus essentially, Pt is acting as catalytic agent for charge transfer between I- and I3- [51]. But, platinum is an expensive and naturally low occurring material so efforts are now aimed at searching for a replacement with cheap and abundantly occurring material. In this context, Carbon is also amongst the most prominent contenders. Many forms of carbon including CNTs [52], graphene [53], meso porous carbon [54], carbon fibers [55], and synthesized carbon [56] had been effectively utilized as CEs with nearly equal or even increased efficiency than platinum. However, adherence to the surface of the substrate and opaque characteristics are the primary issues with carbon based counter electrode materials. Counter electrode materials also include inorganic materials such as sulphides, carbides, and nitrides, as well as organic/inorganic composites [57,58].

2.6 Materials for counter electrodes: an overview

In DSSCs, counter electrode is one the most important component which is usually made up mostly of Pt [59] and a TCO coating on substrate that is serving the function of electron transport layer. Counter Electrode (CE) is required for electron regeneration as well as catalytic reduction of (I^- / I^{3-}) based electrolytes. Pt has a large surface area, better catalytic activity with (I^- / I^{3-}) based electrolytes and outstanding heating behavior and for these reasons, it is chosen as catalyst for CE despite being the most costly component of DSSC [60].

The basis of DSSC technology was built by many significant discoveries from experiments utilizing Pt counter electrodes. But with the aim of increasing solar production all the way to

terawatt scale, Platinum's rare and noble nature, its poor electrolytic stability and high cost has presented a substantial barrier to large scale industrial development and cheaper costs of DSSCs. As a result, the idea and introduction of a Platinum-free CE has recently received a lot of attention. Below is a more thorough discussion of the advances made using Pt and Pt-free counter electrode.

2.6.1 Platinum

Platinum is amongst the most thoroughly investigated counter electrode material for DSSCs technology. For this purpose, a doped substrate (usually fluorine doped tin oxide (FTO)) is used to produce the Pt counter electrode. Different deposition techniques like Sputtering, electro-deposition, chemical reduction, vapor deposition and pyrolysis are just a few of the processes used to make Pt counter electrodes [61-65].

Chemical reduction, in particular, is widely used method because of its ease of use, working at lower temperatures, low platinum loading and strong catalytic activity. The Ma group also looked at the effect of Pt on catalytic activity. A Pt coating with 2nm thickness is adequate for excellent catalytic activity in DSSCs and that Pt films with a thickness of less than 10nm remain transparent. Pt thicknesses greater than 25 nm allow for light reflection, which improves light consumption [66]. On the other hand, Pt's catalytic capacity is linked to the bare facets, which follow the density functional theory (DFT) sequence in which Pt 100 < Pt 411 < Pt 111. [67]. Theoretical calculations and experimental data revealed that Pt 111 oriented CE has best efficiency as compared to Pt 411 or Pt 100 orientations [68]. The recent champion DSSC had achieved the conversion efficiency of 13% utilizing a Pt CE [69].

2.6.2 Carbon Based Counter Electrodes

By utilizing Nano-sized carbon as the counter electrode, Lee and coworkers (2008) [70] achieved a conversion efficiency of approximately 7.16 %. An in-situ carbonization technique was used to manufacture a transparent carbon-based CE with good mechanical stability. The PCE of the bifacial counter electrode was found to be 6.07 % when illuminated from the front and 5.04 % when illuminated from the back. Furthermore, optical properties of carbon-based materials were discovered to be determined by their composition while the electrochemical properties were found to be determined by the concentration of precursor [71]. Veerappan and others (2012) [72] studied spray coated carbon counter electrode with a spray time of 420-seconds. Spray coated

carbon has a photo-conversion efficiency of nearly 6.2 %, according to the researchers. By using carbon-black coated graphite as counter electrode having a layer thickness of 0.2mm, Chen and others (2009) have found power conversion efficiency of 6.56 %, this efficiency is greater than Pt based counter electrode (6.37%) [73].

Wu et al. (2011) employed carbon black, wasted printer toner, carbon fiber, carbon dye, mesoporous carbon, carbon nanotubes, activated carbon, and fullerene as carbonaceous material-based CEs [74]. In comparison to others, mesoporous carbon has a high PCE of 7.5 % when compared with Pt-based CE. Any material's surface area, crystallinity, concentration and composition are all important factors in its effective outcome. The power conversion efficiency of carbon nano-fibers has been investigated at temperatures ranging from 550 to 750 degrees Celsius and found to be greater at 550 degrees Celsius (Sebastián et al., 2014) [75]. Utilizing nitrogen doped mesoporous carbon based CE, a power conversion efficiency of 7.02% was produced by Wang et al. As a result, nitrogen doped mesoporous carbon (NMC) is positioned as the most affordable alternatives to Pt [76]. Jian and others in 2013, reported maximum PCE of 5.65 (%) in DSSC. They used modified mesoporous carbon (MC) as counter electrode. Xu and others in 2018, [77] gathered nineteen different bio wasted carbon materials from Xinyu University campus, China. These bio wasted carbon materials (BCMs) were classified into three categories: (a) seven leaves (b) eleven woods; and (c) two papers: facial tissue and filter paper. After research, they discovered different morphologies are associated with different carbonaceous materials.

Graphene is a two-dimensional carbon molecule having atomically thick sp2 atoms and these atoms are arranged in a honeycomb lattice structure. It has significant promise in a variety of applications, like fuel cells, sensors, super capacitors, and photocatalytic water purification [78, 79-89]. Graphene with conducting polymers has garnered largescale applications in DSSC because it is less expensive, has a good rate of charge transfer with a high catalytic activity [90]. Yue and others (2013) investigated a platinum/graphene film and discovered a power conversion efficiency of 7.78 %. This figure is greater than the platinumt-based conversion efficiency (6.51%). Lin et al. (2017) made Molybdenum Disulphide (MoS2) at room temperature using a straightforward two-step manufacturing method. They used 30 scan cycles to deposit MoS2 on FTO. MoS2/CNTs-3D was created on the surface of one dimensional CNTs by deposition of

MoS2 nanoparticles during hydrophilic treatment. They discovered the maximum PCE of MoS2/CNT-3D nanostructured CE to be 7.82 %, which they attributed to large surface area given by one dimensional CNTs, high catalytic activity of two dimensional MoS2 nanosheets for tri-iodide to iodide reduction in the electrolyte. Although the power conversion efficiency of MoS2/CNTs-3D as counter electrode was above that of platinum counter electrode, it has yet to be commercialized owing to instability concerns [91].

Cationised graphite was created by Mengal and others (2017) by immersion of graphite in the lipase enzyme dispersion. Researchers discovered that inducing fumed silica in the graphite improves the catalytic activity of tri-iodide to iodide reduction by increasing the surface area generated by the nano-spacer. They found that using a hybrid structure as CE boosted graphite's PCE from 4.17 % to 6.19 % [92]. Table 2.1 contains all the important results on carbonaceous based CEs.

Table 2.1 Summary of Important Results on Carbonaceous CEs

Counter Electrode Material	**JSC(mA.cm^{-2})**	**VOC (V)**	**FF**	**PCE(%)**
Carbon Black Powder	11.34	0.825	0.712	6.67
Carbon Black	16.8	0.790	0.685	9.1
Glassy Carbon	19.3	0.662	0.452	5.78
Carbon	16.5	0.0710	0.64	7.56
Transport Carbon	10.54	0.721	0.6	6.07
Graphite – TCO free CE	12	0.816	0.6	5.9
Pure Carbon	13.1	0.703	0.70	6.46
Graphene/Carbon Black	15.07	0.70	0.57	5.99
MoS2/CNTs	16.65	0.74	0.66	7.83
Graphene	13.1	0.7	63.6	5.87

Carbonaceous material has been chosen as a replacement for platinum based counter electrodes due to its inexpensive cost and plentiful availability in nature. Some disadvantages, such as the

carbon films attaches poorly to transparent conducting substrate and the requirement of plentiful availability to achieve the highest catalytic activity limit the long term usage of carbonaceous CEs.

2.6.3 Conducting Polymers as Counter Electrode

By virtue of hard work by researchers, usage of different conducting polymers has been made possible. They have great qualities for decreasing costs, such as fast electron acceleration, cheap and inexpensive, higher stability, and functioning at higher altitudes [93-94]. Among these polymers, polypyrrole, polyaniline (PNI), and 3,4-ethylene dioxythiophene (PEDOT) had previously been used as CE in DSSCs, and they have demonstrated outstanding performance in super capacitor products, water purification and sensors [95]. In these polymers, polyaniline (PNI) has been one of the most researched polymers in the last decade because of its easy manufacturing, environment friendliness, good electrical conductivity, strong redox activity towards iodide and great photocatalytic capability [96,97]. Furthermore, PNI has shown strong photoelectric properties and great catalytic activity for tri-iodide to iodide reduction during redox processes. Laboratory synthesized PNI had a 7.15 % PCE compared to 6.90 (%) for the conventional platinum counter electrode [98-99]. Wu and others (2008) fabricated nanoparticle polypyrole (PPy) coated counter electrode. It was found that PPy electrode had a high rate of charge transfer and a strong catalytic activity for tri-iodide to iodide reduction. Furthermore, the PCE of the PPy CE was reported to be 7.66 % as compared to platinum based counter electrode (6.90%). [100]. When 3,4-ethylene dioxythiophene (PEDOT) was utilized as a counter electrode, it showed excellent electrocatalytic characteristics, high conductivity and durability. Yin and others (2013) created a low-temperature PEDOT counter electrode and obtained a PCE of 7.04% which is comparable to the platinum-based counter electrode (6.90%) [101].

In order to form a poly 3,4 ethylene dioxythiophene (PEDOT) counter electrode, Dai and others used solid state polymerization [102-103]. For polymerization, monomer 2,5-diiodie-3, 4-ethylene dioxythiophene (DIEDOT) were sintered at 135 °C for varios operating hours giving PEDOT-24, PEDOT-36 AND PEDOT-48 FOR 24H, 36H and 48H respectively. After testing, PEDOT-36 gave the highest power conversion efficiency of approximately 6.38% while efficiencies of PEDOT, PEDOT-24 and PEDOT-48 came out to be 4.40%, 6.05%, and 5.57% respectively, by comparison platinum based counter electrode gave an efficiency of 7.35%.

Li and others used another technique for creation of a Pt-free CE. They incorporated reduced graphene oxide (rGO) into different conducting polymers like PNI, PPy, and PEDOT [104] giving a composite of rGO/PNI, rGO/PPy and rGO/PEDOT on a substrate of Ti foil as CE. Power conversion efficiencies of these three were found out to be 5.73%, 6.2% and 4.6% respectively which are also comparable to platinum based counter electrode. Another composite was created by Shih and others using the technique of electrochemical polymerization resulting graphene nanoplatelets(GNP)/polyaniline(PNI)/multiwalled carbonanotubes (MWCNT) or (GNP/PNI/MWCNT) composite. A very high potocurrent conversion efficiency of 7.67% was reported by the researchers which is almost equal to Pt-based counter electrode (7.62%). Furthermore, they showed a strong electocatalytic activity for tri-iodide to iodide reduction and a high rate of charge transfer for the aforementioned composite [105].

2.6.4 Binary metal compounds

Since 2009, a lot of research is aimed at examining binary metal compounds as a substitution for platinum based counter electrode. Sulphides, nitrides, phosphides and carbides are a few types of binary metal compounds.

2.6.4.1 Carbides

Tungsten Carbide (WC) was first employed as CE in carbide based compounds by Lee and others [106]. In addition to WC, molybdenum carbide (MoC) was used by the Ma group [107]. After that, different carbides like VC, Cr3C3, TiC, Ta4C3, NbC, ZrC and SiC were utilized as counter electrodes and their efficiencies were found. They showed strong electrocatalytic activity with exception of ZrC and SiC [108].

2.6.4.2 Sulfides

Cobalt Sulfide (CoS) was the first amongst sulfides which was used as CE because it is inexpensive and abundantly available. By using CoS nanoparticles, Gratzel was able to achieve an efficiency of 6.5% and he also confirmed durability over long-terms, even in very harsh conditions [109]. Since then, there is a lot of interest in CoS CEs. Different sulfide compositions were used as counter electrode including Co_8S_9, CoS nanorods, Co_4S_8, NiS nanoarrays, $Cu_{1.8}S$, Ni_3S_2, Ni_3S_2, FeS_2, and Ni_3S_2 [110-117] in DSSCs. Furthermore, WS_2 and MoS_2 were synthesized and introduced as CEs by Ma group and they exhibited efficiencies of 7.73% and 7.59% for WS_2 and MoS_2 respectively [118].

2.6.4.3 Phosphides

Just like carbides and sulfides, phosphides are also employed as counter electrodes in DSSCs. MoP and Ni_5P_4 phosphides have been synthesized and employed as CEs and their efficiencies were found out to be 4.92% and 5.71% respectively. However, Pt based counter electrodes have shown way more efficiency than phosphides [119]. A lot of opportunity is still available for working on phosphide based counter electrodes.

2.6.4.4 Selenides

Amongst selenides, cobalt selenide ($Co_{0.85}Se$) and nickel selenide ($Ni_{0.85}Se$) were produced as CEs by the Wang group [120]. Counter electrode based on nickel selenide showed an efficiency of 8.23% while that of based on cobalt selenide showed an efficiency of 9.40% which is higher than traditional platinum based counter electrode (7.64%). Similarly, CEs based on CoSe and $NiSe_2$ have also shown efficiencies greater than platinum based CE [121,122]. Moreover, $NbSe_2$ nanorods and nanosheets were produced giving an efficiency comparable to platinum based CE [123].

2.6.4.5 Tellurides

Ma group also manufactured tellurides ($NiTe_2$ and CoTe) and used them as counter electrodes. $NiTe_2$ and CoTe have given efficiencies of 7.21% and 6.92% and these results are very good when comparing wiht Pt-based CEs [124].

2.6.5 Multiple Compounds

Previously, binary compounds have been explained however, various compuounds consisting to three or more than three elements have also been utilized as counter electrodes in DSSCs. One such example is Copper Zinc Tin Sulfide (CZTS) which is first CE based on various elements [125-126]. CZTS nanoparticles and selenized CZTS nanoparticles (CZTSSe) were employed as CEs by Lin group and their work exhibited efficiencies of 3.62% and 7.37% respectively. By optimizing thickness of CZTSe up to 1.2m, the Wu group exhibited an efficiency of 7.82% which is higher than Pt-based CE. Various morphologies of $CuInS_2$ were studied by another group [127] including vertically-oriented nanocrystals and nanosheets of $CuInS_2$. An efficiency of 6.33% was obtained for $CuInS_2$ nanosheets which is nearly equal to that of sputtered Pt-based CE (6.07%) [128]. After the addition of graphite, ternary compounds like $CoMoS_4$, $NiMoS_4$ and $NiCo_2S_4$ also showed efficiencies comparable to Pt when employed as counter electrodes [129, 130].

2.6.6 Composites materials

Counter electrodes based on composite materials are distinct in a way that these are constructed using two or more materials having distinct chemical and/or physical properties. They have a high electrocatalytic activity and are inexpensive, hence they attracted lots of attention. Pt/carbon, MoC/Mesoporous Carbon, TiN/carbon nanotubes, and WC/ordered mesoporous carbon are such composite materials that have been synthesized and tested [131] Furthermore, different composites based on different combinations are made and tested frequently. VC/mesopororus carbon and WO_2/mesoporous carbon were created by Ma group and they showed that these composites happened to have higher catalytic activity than Pt [132,133]. A carbon, polymer and a novel metal system (polypyrrole/C/metal) was created by the Han group and they exhibited better efficiencies using Cobalt, Polypyrrole and Carbon system (Co/polypyrrole/C) (7.639%) and Nickel, Polypyrrole and Carbon system (Ni/polypyrrole/C) (7.439%) than only carbon (6.26%) [134]. Various binary compounds induced with graphene like NiS/graphene CoS/graphene and MoS2/graphene have been presented as CEs [135-136]. Furthermore, multi-walled nanotubes of carbon have also been presented as CEs like MoS2/MWCNTs and WS2/MWCNTs [137, 138]. Single walled carbon nanotubes/reduced graphene oxide (SWCNTs/rGO) is presented as a CE by Ouyang group and they exhibited an efficiency of 8.369%, and this efficiency is greater than platinum-based CE [139].

2.7 Summary

In this chapter, the history of solar cell invention and all the derivation in the way of third generation DSSCs are briefly discussed, as well as all the components of the DSSC have been discussed in detail, their properties, their functions in the cell, and their performance. Normally due to the superior catalytic and conductive properties, pt is taken as standard. Though it showed good performance and high photo conversion efficiencies of the cell, but due to its high cost, different material came into consideration and all the CE materials such as carbonaceous, metal sulphides, metal nitrides, complex conductive polymer, that are being used and been reported, due to their extraordinary properties like highly conductivity, stability and cost effective materials.

2.8 References

[1] Malanima, P., Energy consumption and energy crisis in Roman world. The Ancient Mediterranean Environment between Science and History, 2011: p. 13-36.

[2] Perlin, J., Let it shine: the 6,000-year story of solar energy. 2013: New World Library.

[3] Maruga, N.K., Final year project. 2014. University of Nairobi.

[4] Ruskin, S., John Herschel's Cape voyage: Private science, public imagination and the ambitions of Empire. 2017: Routledge.

[5] Kongtragool, B. and S. Wongwises, A review of solar-powered Stirling engines and low temperature differential Stirling engines. Renewable and Sustainable Energy Reviews, 2003. 7(2): p. 131-154.

[6] Sufian, S.M.A., et al. Design of a Stirling engine to generate green energy in rural areas of Bangladesh. in Green Energy and Technology (ICGET), 2014 2nd International Conference on. 2014. IEEE.

[7] Kolin, I., P. Lista, and V. Naso, The power formula for atmospheric stirling Engines. 1992, SAE Technical Paper.

[8] Grätzel, M., Photoelectrochemical cells. Nature, 2001. 414(6861): p. 338. 25

[9] Timilsina, G. and L. Kurdgelashvili, 25. The evolution of solar energy technologies and supporting policies. Handbook on Geographies of Technology, 2017: p. 362-375.

[10] Ishai, M.B. and F. Patolsky, Shape-and dimension-controlled single-crystalline silicon and SiGe nanotubes: toward nanofluidic FET devices. Journal of the American Chemical Society, 2009. 131(10): p. 3679-3689.

[11] Goetzberger, A. and C. Hebling, Photovoltaic materials, past, present, future. Solar Energy Materials and Solar Cells, 2000. 6 2(1-2): p. 1-19.

[12] Hovel, H.J., Photovoltaic materials and devices for terrestrial solar energy applications. Solar Energy Materials, 1980. 2(3): p. 277-312.

[13] Brown, N., Solar junction breaks concentrated solar world record with 43.5% efficiency. CleanTechnica. com, 2011.

[14] Wanlass, M. W., Single-junction solar cells with the optimum band gap for terrestrial concentrator applications. 1994, Google Patents.

[15] Hubbard, H., Photovoltaics today and tomorrow. Science, 1989. 2 44(4902): p. 297- 304.

[16] Tesla, N., Method of utilizing radiant energy. 1901, Google Patents.

[17] Einstein, A., Does the inertia of a body depend upon its energy-content. Ann Phys, 1905. 18: p. 639-641.

[18] Hegedus, S.S. and A. Luque, Status, trends, challenges and the bright future of solar electricity from photovoltaics. Handbook of Photovoltaic Science and Engineering, 2003: p. 1-43

[19] W. West, “First hundred years of spectral sensitization,” Proc. Vogel Cent. Symp. Photogr. Sci. Eng., vol. 18, pp. 35–48, 1974.

[20] J. Moser, “Notiz über die Verstärkung photoelectrischer Ströme durch optische Sensibilisierung,” Monatsh. Chem., 8, 373, 1887.

[21] Namba, S. & Hishiki, Y., “Color sensitization of zinc oxide with cyanide dyes,” J.Phys. Chem., vol. 69, pp. 774–779, 1965.

[22] W. H. Brattain, C. G. B. Garrett, “Experiments on the interface between germanium and an electrolyte,” Bell Syst. Tech. J., vol. 34, pp. 129–176, 1955.

[23] H. Gerischer, “Electrochemical behavior of semiconductors under illumination,” J.Electrochem. Soc., vol.113, pp. 1174–1182, 1966.

[24] Michael Grätzel, “Review Dye-sensitized solar cells,” Journal of Photochemistry and Photobiology C, Photochemistry Reviews, vol. 4, pp. 145–153, 2003.

[25] H. Xin, J. K. Katahara, I. L. Braly and H. W. Hillhouse, Adv. Energy Mater., 2014, DOI: 10.1002/aenm.201301823.

[26] M. Gratzel, Nature, 2001, 414,338-344.

[27] B. O’Regan and M. Gratzel, Nature, 1991, 353, 737–740

[28] A. Stadler, Materials**, 2012**, 5, 661-683.

[29] T. Minami, T.Miyata, T. Yamamoto, Surface and Coatings Technology, **1998**, 10, 583–587.

[30] B. O'Regan, M. Grätzel, Nature, 1991, 353, 737–740.

[31] K Keis, E.Magnusson, H. Lindstrom, S.E. Lindquist, A. Hagfeldt, Solar Energy Materials and Solar Cells , 2002,73,51–8.

[32] M.Saito, S. Fujihara, Energy Environ. Sci., 2008, 1, 280–3.

[33] E. Ramasamy, J. Lee, J. Phys Chem. C, 2010, 114, 22032–7.

[34] G.A Parks., Chem Rev., 1965, 65,177–98.

[35] L.Huang, L. Jiang, M. Wei, Electrochem. Comm., 2010, 12, 319–22

[36] T. G. Deepak, G. S. Anjusree, S. Thomas, T. A. Arun, S. V. Nair and A. Sreekumaran Nair, RSC Adv., 2014, 4, 17615-17638.

[37] L. Zhao, J. Li, Y. Shi, S. Wang, J. Hu, B. Dong, H. Lu and P. Wang, J. Alloy. Compd., 2013, 575, 168-173.

[38] J. Qi, X. Dang, P. T. Hammond and A. M. Belcher, ACS Nano, 2011, 5, 7108- 7116.

[39] X. Kou, S. Zhang, C.-K. Tsung, Z. Yang, M. H. Yeung, G. D. Stucky, L. Sun, J. Wang and C. Yan, Chem.-Eur. J., 2007, 13, 2929-2936.

[40] W. Ni, X. Kou, Z. Yang and J. Wang, ACSNano, 2008, 2, 677-686.

[41] Z. Sun, J. H. Kim, Y. Zhao, D. Attard and S. X. Dou, Chem. Commun., 2013, 49, 966-968.

[42] Z. Dong, H. Ren, C. M. Hessel, J. Wang, R. Yu, Q. Jin, M. Yang, Z. Hu, Y. Chen, Z. Tang, H. Zhao and D. Wang, Adv. Mater., 2014, 26, 905-909.

[43] L. De Marco, M. Manca, R. Giannuzzi, M. R. Belviso, P. D. Cozzoli and G. Gigli, EnergyEnviron. Sci., 2013, 6, 1791-1795.

[44] G. Calogero, G.D. Marco, S.Caramori, S.Cazzanti, R. Argazzi, C. Bignozzi, Energy Environ. Sci., 2009, 2, 1162–1172.

[45] M. Liang and J. Chen, Chem. Soc. Rev., 2013, 42, 3453-3488.

[46] Y.-S. Yen, H.-H. Chou, Y.-C. Chen, C.-Y. Hsu and J. T. Lin, J. Mater. Chem., 2012, 22, 8734-8747.

[47] S. Ahmad, E. Guillen, L. Kavan, M. Grätzel and M. K. Nazeeruddin, Energy Environ. Sci., 2013, 6, 3439-3466.

[48] A.Yella, H-W. Lee, H.N.Tsao, C. Yi, A.K. Chandiran, M.K. Nazeeruddin, E.D. WeiGuang, C-Y.Yeh, S.M. Zakeeruddin, M. Grätzel, Science, 2011, 3344.

[49] S. Y. Huang, G. Schlichthorl , A. J. Nozik, M. Gratzel, A.J. Frank Journal of Physical Chemistry B ,1997,101,2576–82.

[50] T. Daeneke, Y. Uemura, NW. Duffy, AJ. Mozer, N. Koumura, U. Bach, L. Spiccia, Advanced Materials, 2012,24, 1222-1225.

[51] M. Wu and T. Ma, ChemSusChem , 2012, 5, 1343 – 1357.

[52] W. J. Lee, E. Ramasamy, D. Y. Lee, J. S. Song, ACS Appl. Mater. Interfaces, 2009, 1, 1145- 1149.

[53] J. D. R.-Mayhew, D. J. Bozym, C. Punckt, and I.A. Aksay, ACS Nano, 2010,4, 6203-6211.

[54] E. Ramasamy, J. Lee, Carbon, 2010, 48, 3715-3720.

[55] J. D. Roy-Mayhew, D. J. Bozym, C. Punckt, I. A. Aksay, ACS Nano, 2010,4, 6203.

[56] E. Ramasamy, J. Lee, Carbon, 2010, 48, 3715

[57] H.K. Mulmudi, S. K. Batabyal, M. Rao,R. R. Prabhakar, N. Mathews, Y- M Lam and S. G. Mhaisalkar, Phys. Chem. Chem. Phys., 2011, 13, 19307–19309.

[58] Calandra P, Calogero G,Sinopoli A, Gucciardi P G, Catalyst, 2010;3:4a.

[59] Tang, Z., Wu, J., Zheng, M., Huo, J., Lan, Z., 2013. A microporous platinum counter electrode used in dye-sensitized solar cells. Nano Energy 2, 622 –627.

[60] Lee, Y.-L., Chen, C.-L., Chong, L.-W., Chen, C.-H., Liu, Y.-F., Chi, C.-F., 2010. A platinum counter electrode with high electrochemical activity and high transparency for dyesensitized solar cells. Electrochem. Commun. 12, 1662 –1665.

[61] P. Li, J. Wu, J. Lin, M. Huang, Z. Lan and Q. Li, Electrochim. Acta, 2008, 53, 4161-4166.

[62] G. Wang, R. Lin, Y. Lin, X. Li, X. Zhou and X. Xiao, Electrochim. Acta, 2005, 50, 5546-5552.

[63] M. Ikegami, K. Miyoshi, T. Miyasaka, K. Teshima, T. C. Wei, C. C. Wan and Y. Y. Wang, Appl. Phys. Lett., 2007, 90, 153122.

[64] E. Olsen, G. Hagen and S. Eric Lindquist, Sol. Energy Mater. Sol. Cells, 2000, 63, 267-273.

[65] L. Chen, W. Tan, J. Zhang, X. Zhou, X. Zhang and Y. Lin, Electrochim. Acta, 2010, 55, 3721-3726.

[66] X. Fang, T. Ma, G. Guan, M. Akiyama, T. Kida and E. Abe, J. Electroanal. Chem., 2004, 570, 257-263.

[67] B. Zhang, D. Wang, Y. Hou, S. Yang, X. H. Yang, J. H. Zhong, J. Liu, H. F. Wang, P. Hu, H. J. Zhao and H. G. Yang, Sci. Rep., 2013, 3, 1386.

[68] R. Narayanan and M. A. El-Sayed, Nano Lett., 2004, 4, 1343-1348. 107

[69] S. Mathew, A. Yella, P. Gao, R. Humphry-Baker, F. E. CurchodBasile, N. AshariAstani, I. Tavernelli, U. Rothlisberger, K. NazeeruddinMd and M. Grätzel, Nat Chem, 2014, 6, 242-247.

[70] Lee, W.J., Ramasamy, E., Lee, D.Y., Song, J.S., 2008. Performance variation of carbon counter electrode based dye-sensitized solar cell. Sol. Energy Mater. Sol. Cells 92, 814 –818.

[71] Bu, C., Liu, Y., Yu, Z., You, S., Huang, N., Liang, L., et al., 2013. Highly transparent carbon counter electrode prepared via an in-situ carbonization method for bifacial dye sensitized solar cells. ACS Appl. Mater. Interfaces 5, 7432 –7438

[72] Veerappan, G., Bojan, K., Rhee, S.-W., 2012. Amorphous carbon as a flexible counter electrode for low cost and efficient dye sensitized solar cell. Renew. Energy 41,383 –388.

[73] Veerappan, G., Bojan, K., Rhee, S.-W., 2011. Sub-micrometer-sized graphite as a conducting and catalytic counter electrode for dye-sensitized solar cells. ACS Appl. Mater. Interfaces 3, 857 –862.

[74] Chen, J., Li, K., Luo, Y., Guo, X., Li, D., Deng, M., et al., 2009. A flexible carbon counter electrode for dye-sensitized solar cells. Carbon 47, 2704 –2708.

[75] Wu, M., Lin, X., Wang, T., Qiu, J., Ma, T., 2011. Low-cost dye-sensitized solar cell based on nine kinds of carbon counter electrodes. Energy Environ. Sci. 4, 2308 –2315.

[76] Sebastián, D., Baglio, V., Girolamo, M., Moliner, R., Lázaro, M., Aricò, A., 2014. Carbon nanofiber-based counter electrodes for low-cost dye-sensitized solar cells. J. Power Sources 250, 242 –249.

[77] Wang, G., Kuang, S., Wang, D., Zhuo, S., 2013. Nitrogen-doped mesoporous carbon as low-cost counter electrode for high-efficiency dye-sensitized solar cells. Electrochim.Acta 113, 346 –353.

[78] Xu, S., Liu, C., Wiezorek, J., 2018. 20 renewable biowastes derived carbon materials as green counter electrodes for dye-sensitized solar cells. Mater. Chem. Phys. 204, 294 –304.

[79] Ikhsan, N.I., Rameshkumar, P., Pandikumar, A., Shahid, M.M., Huang, N.M., Kumar, S.V., et al., 2015. Facile synthesis of graphene oxide –silver nanocomposite and its modified electrode for enhanced electrochemical detection of nitrite ions. Talanta 144, 908 –914

[80] Shahid, M.M., Pandikumar, A., Golsheikh, A.M., Huang, N.M., Lim, H.N., 2014. Enhanced electrocatalytic performance of cobalt oxide nanocubes incorporating reduced graphene oxide as a modified platinum electrode for methanol oxidation. RSC Adv. 4, 62793 –62801.

[81] Shahid, M.M., Rameshkumar, P., Huang, N.M., 2015. Morphology dependent electrocatalytic properties of hydrothermally synthesized cobalt oxide nanostructures. Ceram. Int. 41, 13210–13217.

[82] Shahid, M.M., Rameshkumar, P., Pandikumar, A., Lim, H.N., Ng, Y.H., Huang, N.M., 2015. An electrochemical sensing platform based on a reduced graphene oxide –cobalt oxide nanocube@ platinum nanocomposite for nitric oxide detection. J.Mater.Chem.A3,14458–14468.

[83] Shahid, M.M., Rameshkumar, P., Huang, N.M., 2016. A glassy carbon electrode modified

with graphene oxide and silver nanoparticles for amperometric determination of hydrogen peroxide. Microchim. Acta 183, 911 –916.

[84] Shahid, M.M., Rameshkumar, P., Basirunc, W.J., Wijayantha, U., Chiu, W.S., Khiew, P.S., et al., 2018. An electrochemical sensing platform of cobalt oxide@ gold nanocubes interleaved reduced graphene oxide for the selective determination of hydrazine. Electrochim. Acta 259, 606 –616.

[85] Numan, A., Shahid, M.M., Omar, F.S., Rafique, S., Bashir, S., Ramesh, K., et al., 2017. Binary nanocomposite based on Co3O4 nanocubes and multiwalled carbon nanotubes as an ultrasensitive platform for amperometric determination of dopamine. Microchim. Acta 184, 2739 –2748.

[86] Yusoff, N., Rameshkumar, P., Mehmood, M.S., Pandikumar, A., Lee, H.W., Huang, N.M.,2017. Ternary nanohybrid of reduced graphene oxide-nafion@ silver nanoparticlesfor boosting the sensor performance in non-enzymatic amperometric detection ofhydrogen peroxide. Biosens. Bioelectron. 87, 1020 –1028.

[87] Yusoff, N., Rameshkumar, P., Shahid, M.M., Huang, S.-T., Huang, N.M., 2017.Amperometric detection of nitric oxide using a glassy carbon electrode modified with gold nanoparticles incorporated into a nanohybrid composed of reduced graphene oxide and Nafion. Microchim. Acta 184, 3291 –3299.

[88] Chang, B.Y.S., Mehmood, M.S., Pandikumar, A., Huang, N.M., Lim, H.N., Marlinda, A.R., et al., 2016. Hydrothermally prepared graphene-titania nanocomposite for the solar photocatalytic degradation of methylene blue. Desalin. Water Treat. 57, 238 –245.

[89] Anuar, N.S., Basirun, W.J., Ladan, M., Shalauddin, M., Mehmood, M.S., 2018. Fabrication of platinum nitrogen-doped graphene nanocomposite modified electrode for the electrochemical detection of acetaminophen. Sens. Actuators, B 266, 375 –383.

[90] Stankovich, S., Dikin, D.A., Dommett, G.H., Kohlhaas, K.M., Zimney, E.J., Stach, E.A., et al., 2006. Graphene-based composite materials. Nature 442, 282.

[91] Lin, C.-H., Tsai, C.-H., Tseng, F.-G., Ma, C.-C.M., Wu, H.-C., Hsieh, C.-K., 2017. Threedimensional vertically aligned hybrid nanoarchitecture of two-dimensional molybdenum

disulfide nanosheets anchored on directly grown one-dimensional carbon nanotubes for use as a counter electrode in dye-sensitized solar cells. J. Alloy. Compd. 692, 941 –949.

[92] Mengal, N., Arbab, A.A., Memon, A.A., Sahito, I.A., Jeong, S.H., 2017. A promising hybrid graphite counter electrode doped with fumed silica nano-spacers for efficient quasisolid state dye sensitized solar cells. Electrochim. Acta.

[93] Jeon, S.S., Kim, C., Ko, J., Im, S.S., 2011. Spherical polypyrrole nanoparticles as a highly efficient counter electrode for dye-sensitized solar cells. J. Mater. Chem. 21, 8146 –8151.

[94] Rafique, S., Abdullah, S.M., Shahid, M.M., Ansari, M.O., Sulaiman, K., 2017. Significantly improved photovoltaic performance in polymer bulk heterojunction solar cells with graphene oxide/PEDOT: PSS double decked hole transport layer. Sci. Rep. 7, 39555.

[95] Omar, F.S., Numan, A., Duraisamy, N., Ramly, M.M., Ramesh, K., Ramesh, S., 2017. Binary composite of polyaniline/copper cobaltite for high performance asymmetric supercapacitor application. Electrochim. Acta 227, 41 –48.

[96] Kang, E., Neoh, K., Tan, K., 1998. Polyaniline: a polymer with many interesting intrinsic redox states. Prog. Polym. Sci. 23, 277 –324.

[97] Syed, S., 2016. Polyaniline based Nanocomposites as Adsorbents and Photocatalysts in the Removal of Organic Dyes/Syed Shahabuddin. University of Malaya.

[98] Li, Q., Wu, J., Tang, Q., Lan, Z., Li, P., Lin, J., et al., 2008. Application of microporous polyaniline counter electrode for dye-sensitized solar cells. Electrochem. Commun. 10, 1299 –1302.

[99] Xiao, Y., Han, G., Li, Y., Li, M., Chang, Y., 2014. High performance of Pt-free dye-sensitized solar cells based on two-step electropolymerized polyaniline counter electrodes. J. Mater. Chem. A 2, 3452 –3460

[100] Wu, J., Li, Q., Fan, L., Lan, Z., Li, P., Lin, J., et al., 2008. High-performance polypyrrole nanoparticles counter electrode for dye-sensitized solar cells. J. Power Sources 181, 172 –176.

[101] Yin, X., Wu, F., Fu, N., Han, J., Chen, D., Xu, P., et al., 2013. Facile synthesis of poly (3, 4- ethylenedioxythiophene) film via solid-state polymerization as high-performance Ptfree

counter electrodes for plastic dye-sensitized solar cells. ACS Appl. Mater. Interfaces 5, 8423 –8429.

[102] udhagar, P., Nagarajan, S., Lee, Y.-G., Song, D., Son, T., Cho, W., et al., 2011. Synergistic catalytic effect of a composite (CoS/PEDOT: PSS) counter electrode on triiodide reduction in dye-sensitized solar cells. ACS Appl. Mater. Interfaces 3, 1838 –1843.

[103] Dai, X., Li, A., Wu, F., Xie, A., 2016. Solid-state synthesis of a conducting polythiophene as efficient Pt-free thin film counter electrode for dye-sensitized solar cells. Mater. Lett. 174, 91 –94.

[104] Li, R., Tang, Q., Yu, L., Yan, X., Zhang, Z., Yang, P., 2016. Counter electrodes from conducting polymer intercalated graphene for dye-sensitized solar cells. J. Power Sources 309, 231 –237

[105] Shih, Y.-C., Lin, H.-L., Lin, K.-F., 2017. Electropolymerized polyaniline/graphene nanoplatelet/multi-walled carbon nanotube composites as counter electrodes for high performance dye-sensitized solar cells. J. Electroanal. Chem. 794, 112 –119.

[106] J. S. Jang, D. J. Ham, E. Ramasamy, J. Lee and J. S. Lee, Chem. Commun., 2010, 46, 8600-8602.

[107] M. Wu, X. Lin, A. Hagfeldt and T. Ma, Angew. Chem.-Int. Edit., 2011, 50, 3520- 3524.

[108] G. R. Li, J. Song, G. L. Pan and X. P. Gao, Energy Environ. Sci., 2011, 4, 1680- 1683.

[109] M. Wang, A. M. Anghel, B. Marsan, N.-L. Cevey Ha, N. Pootrakulchote, S. M. Zakeeruddin and M. Grätzel, J. Am. Chem. Soc., 2009, 131, 15976-15977.
[110] S.-H. Chang, M.-D. Lu, Y.-L. Tung and H.-Y. Tuan, ACS Nano, 2013, 7, 9443- 9451.

[111] C.-W. Kung, H.-W. Chen, C.-Y. Lin, K.-C. Huang, R. Vittal and K.-C. Ho, ACS Nano, 2012, 6, 7016-7025.

[112] H. Sun, D. Qin, S. Huang, X. Guo, D. Li, Y. Luo and Q. Meng, Energy Environ. Sci., 2011, 4, 2630-2637.

[113] W. Zhao, X. Zhu, H. Bi, H. Cui, S. Sun and F. Huang, J. Power Sources, 2013, 242, 28-32.
108

[114] H. K. Mulmudi, S. K. Batabyal, M. Rao, R. R. Prabhakar, N. Mathews, Y. M. Lam and S. G. Mhaisalkar, Phys. Chem. Chem. Phys., 2011, 13, 19307-19309.

[115] H. Zhang, L. Yang, Z. Liu, M. Ge, Z. Zhou, W. Chen, Q. Li and L. Liu, J. Mater. Chem., 2012, 22, 18572-18577.

[116] Y.-C. Wang, D.-Y. Wang, Y.-T. Jiang, H.-A. Chen, C.-C. Chen, K.-C. Ho, H.-L. Chou and C.-W. Chen, Angew. Chem.-Int. Edit., 2013, 52, 6694-6698.

[117] Q.-H. Huang, T. Ling, S.-Z. Qiao and X.-W. Du, J. Mater. Chem. A, 2013, 1, 11828-11833.

[118] M. Wu, Y. Wang, X. Lin, N. Yu, L. Wang, L. Wang, A. Hagfeldt and T. Ma, Phys. Chem. Chem. Phys., 2011, 13, 19298-19301.

[119] M. Wu, J. Bai, Y. Wang, A. Wang, X. Lin, L. Wang, Y. Shen, Z. Wang, A. Hagfeldt and T. Ma, J. Mater. Chem., 2012, 22, 11121-11127.

[120] F. Gong, H. Wang, X. Xu, G. Zhou and Z.-S. Wang, J. Am. Chem. Soc., 2012, 134, 10953-10958.

[121] F. Gong, X. Xu, Z. Li, G. Zhou and Z.-S. Wang, Chem. Commun., 2013, 49, 1437-1439.

[122] Z. Zhang, S. Pang, H. Xu, Z. Yang, X. Zhang, Z. Liu, X. Wang, X. Zhou, S. Dong, X. Chen, L. Gu and G. Cui, RSC Adv., 2013, 3, 16528-16533.

[123] J. Guo, Y. Shi, C. Zhu, L. Wang, N. Wang and T. Ma, J. Mater. Chem. A, 2013, 1, 11874-11879.

[124] J. Guo, Y. Shi, Y. Chu and T. Ma, Chem. Commun., 2013, 49, 10157-10159.

[125] X. Xin, M. He, W. Han, J. Jung and Z. Lin, Angew. Chem.-Int. Edit., 2011, 50, 11739-11742.

[126] J. Wang, X. Xin and Z. Lin, Nanoscale, 2011, 3, 3040-3048. 109

[127] S.-J. Yuan, Z.-J. Zhou, Z.-L. Hou, W.-H. Zhou, R.-Y. Yao, Y. Zhao and S.-X. Wu, Chem.-Eur. J., 2013, 19, 10107-10110.

[128] J. Yang, C. Bao, J. Zhang, T. Yu, H. Huang, Y. Wei, H. Gao, G. Fu, J. Liu and Z. Zou, Chem. Commun., 2013, 49, 2028-2030.

[129] J.-Y. Lin and S.-W. Chou, Electrochem. Commun., 2013, 37, 11-14. 78. X. Zheng, J. Guo, Y. Shi, F. Xiong, W.-H. Zhang, T. Ma and C. Li, Chem. Commun., 2013, 49, 9645-9647.

[130] M. Wu and T. Ma, ChemSusChem, 2012, 5, 1343-1357.

[131] M. Wu, X. Lin, Y. Wang, L. Wang, W. Guo, D. Qi, X. Peng, A. Hagfeldt, M. Grätzel and T. Ma, J. Am. Chem. Soc., 2012, 134, 3419-3428.

[132] M. Wu, X. Lin, L. Wang, W. Guo, Y. Wang, J. Xiao, A. Hagfeldt and T. Ma, TheJ. Phys. Chem. C, 2011, 115, 22598-22602.

[133] G. Liu, X. Li, H. Wang, Y. Rong, Z. Ku, M. Xu, L. Liu, M. Hu, Y. Yang and H. Han, J. Mater. Chem. A, 2013, 1, 1475-1480.

[134] J.-Y. Lin, G. Yue, S.-Y. Tai, Y. Xiao, H.-M. Cheng, F.-M. Wang and J. Wu, Mater. Chem. Phys.,2013, 143, 53-59.

[135] J.-Y. Lin, C.-Y. Chan and S.-W. Chou, Chem. Commun., 2013, 49, 1440-1442.

[136] H. Bi, W. Zhao, S. Sun, H. Cui, T. Lin, F. Huang, X. Xie and M. Jiang, Carbon, 2013, 61, 116-123.

[137] G. Yue, J. Wu, J.-Y. Lin, Y. Xiao, S.-Y. Tai, J. Lin, M. Huang and Z. Lan, Carbon, 2013, 55, 1-9.

[138] S.-Y. Tai, C.-J. Liu, S.-W. Chou, F. S.-S. Chien, J.-Y. Lin and T.-W. Lin, J. Mater. Chem., 2012, 22, 24753-24759.

[139] H. Zheng, C. Y. Neo and J. Ouyang, ACS Appl. Mater. Interfaces, 2013, 5, 6657- 6664. 110

Chapter 3: Methodology

As a renowned porous material, activated carbon having a large pore volume and surface area offers a variety of applications such as "gas separation, solvent recovery, wastewater treatments, and purification of water and can act as catalyst in energy conversion and storage processes [1]. In this regard, both synthetic and natural materials of different types like fossil fuels primarily coal, and biomass-based materials like wood, agricultural waste, or industrial waste are

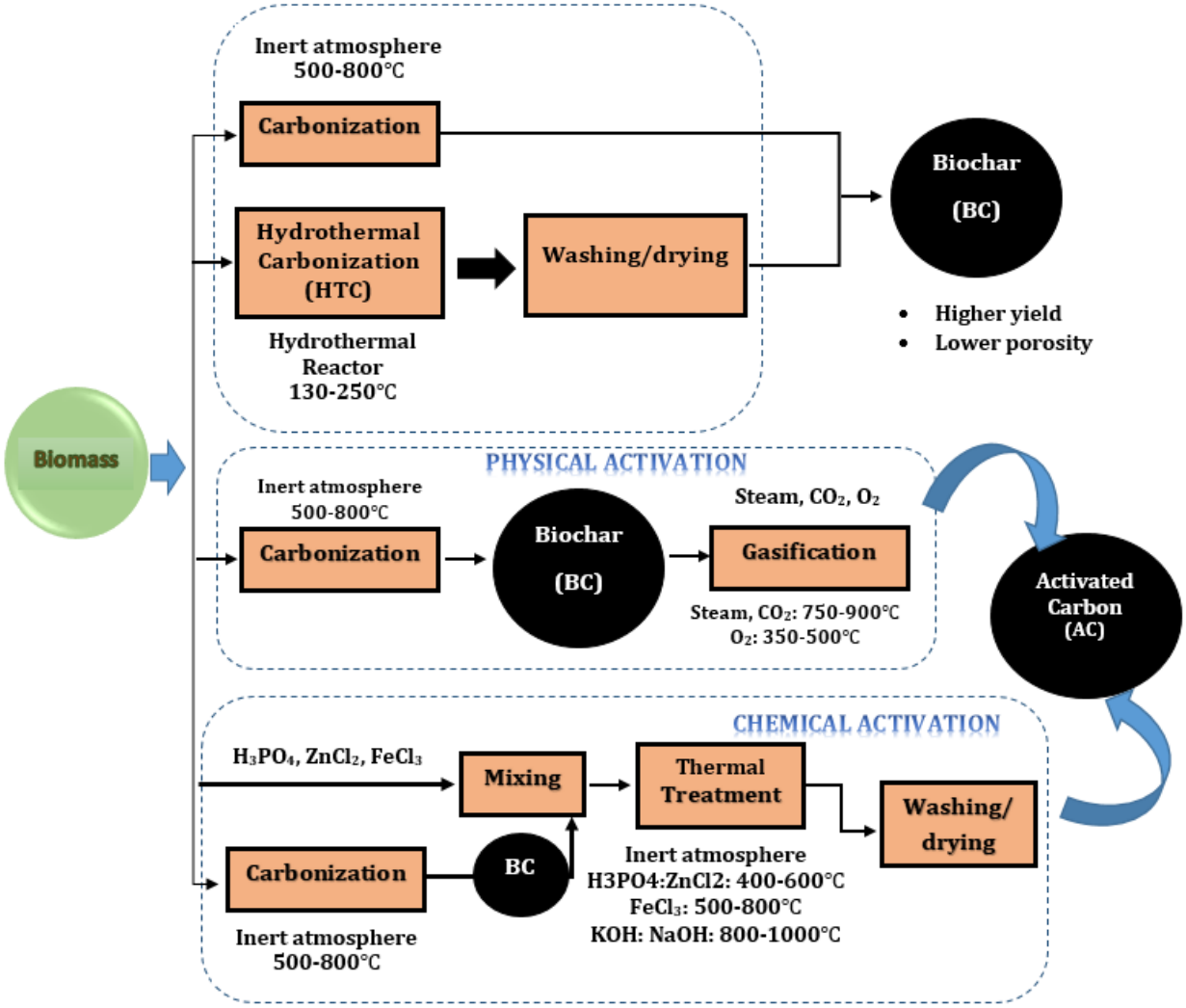

Figure 3-1 Pathways for synthesis of activated carbon

employed as precursors to produce activated carbon.

Among them biomass material has earned the significant attention of scientists and researchers as being renewable, abundant, low cost, and environment friendly. Production of activated carbonaceous materials from biomass can be carried out by adopting either chemical or physical activation processes. Before the chemical or physical activation processes, precursor materials (carbon) are subjected to the carbonization process. The outcome of the carbonization process is termed carbonized material, char, and specifically biochar (BC) if the precursor material is derived from biomass. Figure 3.1 summarize the synthetic paths in production of activated carbon.

Among biomass, hemp bast fiber can be utilized as feedstock for Biochar production as it possesses a multilevel layered structure composed of lignin, hemicellulose, and cellulose biopolymers. Secondly, the ease of its cultivation without any specific requirements like fertilizers, pesticides, and the climate makes it a suitable candidate for this purpose. In the current study, we have also used hemp leaves as biomass precursor material to obtain activated carbon.

3.1 Methods

3.1.1 Synthesis of Hemp-Based Activated Carbon

During pre-treatment steps, hemp leaves were initially separated thoroughly followed by cleaning and washing. Consecutively, the hemp leaves were subjected to complete drying in an oven at 80℃ and were finally grounded in mortar and pestle. For achieving a specific particle size, the grounded hemp powder was sieved out through the 0.6mm mesh.

The carbonization was carried out in a tube furnace (GSL-1800X, MTI corporation) at 750℃ for two hours. With the heating rate of 10℃/minute and inert atmosphere with 40 ml min^{-1} N2 gas flow the dried hemp powder was heated at 750℃ for two hours. The resultant product was designated as Biochar (BC).

In the chemical activation process, 10 mL of hydrogen peroxide (with 30% purity) was mixed with 1.0 grams of Biochar. At room temperature, the whole mixture was kept under constant stirring for about 6h. Afterwards, the product was washed multiple times thoroughly using distilled water until it became free from runoff of impurities. The modified material was dried

overnight in the oven at 110℃. The product obtained after this step was termed activated carbon (AC) [3]. Fig. 3.2 represents the schematic route of activated carbon synthesis.

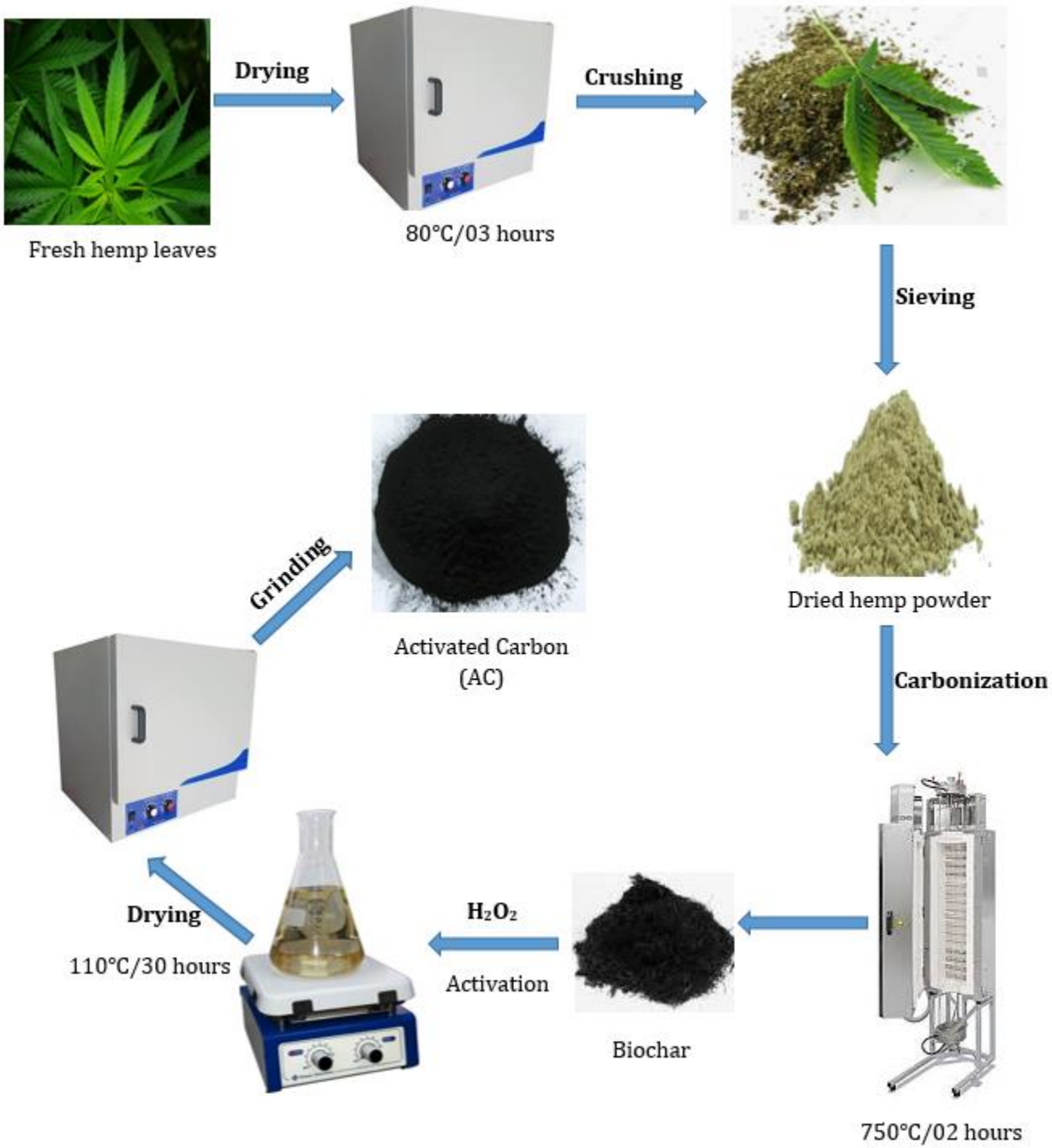

Figure 3-2 Scheme for the formation of activated carbon from hemp-based biomass

The fabrication of a CE for DSSC was done by preparing the slurry of activated carbon. For this purpose, ethanol was used as the solvent, and to avoid agglomeration of very fine carbon particles (AC) that were obtained as the final product in the previous step, polyvinylpyrrolidone PVP (Sigma Aldrich, K-32) was added as surfactant.

Firstly, a homogenous solution of PVP and ethanol (AR grade) was prepared by constant stirring for about thirty minutes. To the solution of PVP, activated carbon was added and the entire mixture was placed on a pot mill for 02 days, so that a homogenous slurry may be formed by de-agglomeration of fine powder. The weight ratio of carbon to PVP was kept at 8:1[4]. Doctor blade coating technique as employed before [5], was used to coat the slurry on the FTO-glass substrate during the fabrication of the counter electrode. 3M scotch tape was utilized for coating purposes on the area of interest. To wear out the binder, the counter electrode was placed in a furnace in a flowing argon atmosphere for 60 minutes at 450℃.

3.1.2 Preparation of the Photo anode

Doctor blade coating technique was also used in the fabrication of photoanode. To develop the TiO_2 (Degussa P25, Sigma Aldrich) based photoanodes, 2g of TiO2 were mixed with 15mL of ethanol to form a paste while stirring. To this a drop of nitric acid and 1mL of distilled water were added and the entire mixture was stirred for 5 hours. On ITO coated-glass substrates (KINTEC, Hong Kong, dimensions 2.5 X 2.5 cm^2, 1.1 mm thick, sheet resistance of 378 **Ω**/sq.) thin film of the above-prepared slurry was formed using doctor blade technique. These prepared samples were dried followed by annealing at 450℃. 0.5mM solution of solaronix N-719 dye was prepared and to this solution previously prepared, semiconductor electrodes were dipped for twenty four hours at room temperature. After that, ethanol and water were used to thoroughly wash the photoanodes [6].

3.1.3 Fabrication of Dye-Sensitized Solar Cell

With the help of clipper pins, fabricated counter electrodes (CEs) were clipped together to sandwich the photoanodes. In between the photoanode and counter electrodes, an electrolyte solution was introduced. For making the electrolyte solution, 500mM 4-tert-butylpyridine and 100mM tetramethylammonium iodide were stirred together along with 100mM tetrabutylammonium iodide. To this 100mM lithium iodide, 100mM potassium iodide, and 50mLof acetonitrile was also added [6].

3.2 Characterization

In order to study the morphology and texture of fabricated CEs, Field Emission Scanning Electron Microscope (FESEM) ***FEI Quanta 400*** at 5kV voltage. In Fourier Transform infrared Spectroscopy technique, the FTIR spectrum of all materials including precursor powdered hemp was recorded on ***Perkin Elmer FTIR spectrum 400*** for specific functional and structural groups over a wavenumber range from 4000-650 cm^{-1}. Measurements on Raman spectroscopy were performed on the instrument. X-ray diffraction (XRD) measurements were recorded and analyzed using PAN analytical X'pert High Score Diffractometer by operating the instrument at 40mA current and 10 kV voltage with the step size of 0.026^0/s in the 2Ɵ range from 10^0-90^0.

For cyclic voltammetry (CV) studies, an electrochemical cell system of three electrodes called PAR-Versa STAT electrochemical workstation was used. As a working electrode, the prepared carbon counter electrode was used along with Ag/AgCl electrode as the reference electrode. In CV, the supporting electrolyte solution was prepared in acetonitrile and it consisted of 500mM $LiClO_4$, 10mM I_2, and 50mM LiI.

3.3 Summary

In the chapter 3 synthesizing, fabrication and characterization have been discussed related to the CE material for the DSSC applications. In synthesize techniques, the different methods and different processes are adopted to make the CE material with their advantages and disadvantages and which technique is more preferred over others. In fabrication process, different coating methods are being used to coat the sample paste with the volatile solvent over the surface of the substrates to form thin films with controlled thickness. Last but not least, after fabricating the CE material, the prepared samples of CE were characterized through various techniques from material structure identification, material morphology to electrocatalytic activity to know the material property and behave towards the solar cell applications.

3.4 References

[1]. A. Jain, R. Balasubramanian and M. Srinivasan, Hydrothermal conversion of biomass waste to activated carbon with high porosity: a review, Chemical Engineering Journal. 2016, 283(1), 789-8.5.

[2]. J. Bedia, M.Penas-Garzon, A. Gomez-Aviles and J.J. Rodriguez and C. Belver, A Review on the Synthesis and Characterization of Biomass-Derived Carbons for Adsorption of Emerging Contaminants from Water, C-Journal of Carbon Research. 2018, 4(4):63, 01-53.

[3]. M. A. Munawar, A.H. Khoja, M. Hassan, R. Liaquat, S.R. Naqvi, M.T. Mehran, A. Abdullah and F. Saleem, Biomass Ash Characterization, Fusion Analysis and Its Application in Catalytic Decomposition of Methane. Fuel, 2021, 285 (1), 119107.

[4]. R.Kumar, S.S. Nemala, S. Mallick and P. Bhargava, Synthesis and Characterization of Carbon Based Electrode for Dye Sensitized Solar Cells (DSSCs) Using Sugar free as a Carbon Material, Solar Energy, 2017, 144(1), 215-220.

[5]. S. Shakir, Z.S. Khan, A. Ali, N. Akbir and W. Mushtaq, Development of Copper Doped Titania based Photoanode and its Performance for Dye Sensitized Solar Cell Applications, Journal of Alloys and Compounds, 2015, 652(1), 331-340.

[6]. S. Shakir, Y.Y. Foo,N. Rizan, H. M. Abdur-ur-Rehman, K. Yunus, P.S. Moi and V. Periasamy, Electro-Catalytic and Structural Studies of DNA Templated Gold Wires on Platinum/ITO as Modified Counter Electrode in Dye Sensitized Solar Cells, Journal of Material Science: Materials in Electronics,2018, 29(1), 4602-4611.

Chapter 4: Results and Discussions

Hemp-derived activated carbon was synthesized and used as a carbonaceous counter electrode for the fabrication of Dye-sensitized solar cells. For the structural elucidation and to examine the morphology, as well as certain other physiochemical properties, the detail characterization of the prepared material, was carried out.

4.1 Raman Spectroscopic Analysis

Raman spectroscopy was used to assess the carbon structure, porosity, ordered and disordered crystal structures of the hemp-derived activated carbon. To find out the development of microstructures like graphite, Raman spectroscopy is used as this technique is highly sensitive to sp2 carbon structures [1, 2, and 3].

For all those biochars, carbonized at a temperature of 600°C and above two important and main peaks are used to appear in the Raman spectrum. The one peak is placed at 1579-1594 cm^{-1} and is designated as **G-band** while the second one is placed at 1298-1321 cm^{-1} and is usually called the **D-band.** Figure 4.1 compares the Raman spectra of hemp-derived activated carbon samples and conventional carbon samples.

It is evident from the figure that the interaction of stacked graphene layers is also present and is marked by the appearance of a 2D band between 2500 to 2900 cm^{-1}[4]. Escribano and the co-workers reported that the presence of a strong and narrow 2D band in the spectra characterized the ordered carbon material whereas the weak and broadband is the representative of carbon material with extensively disordered structure or having very small crystal size. In our case, the presence of a strong and narrow 2D band along with distinct G and D bands suggest that a highly crystalline and ordered carbon structure has been formed. The structure of commercially activated carbon (C-12 from fig 4.1) exhibits similar Raman shifts thus indicating the same structures. Hence, our material (HAC) is in the agreement with the conventional activated carbon material [5].

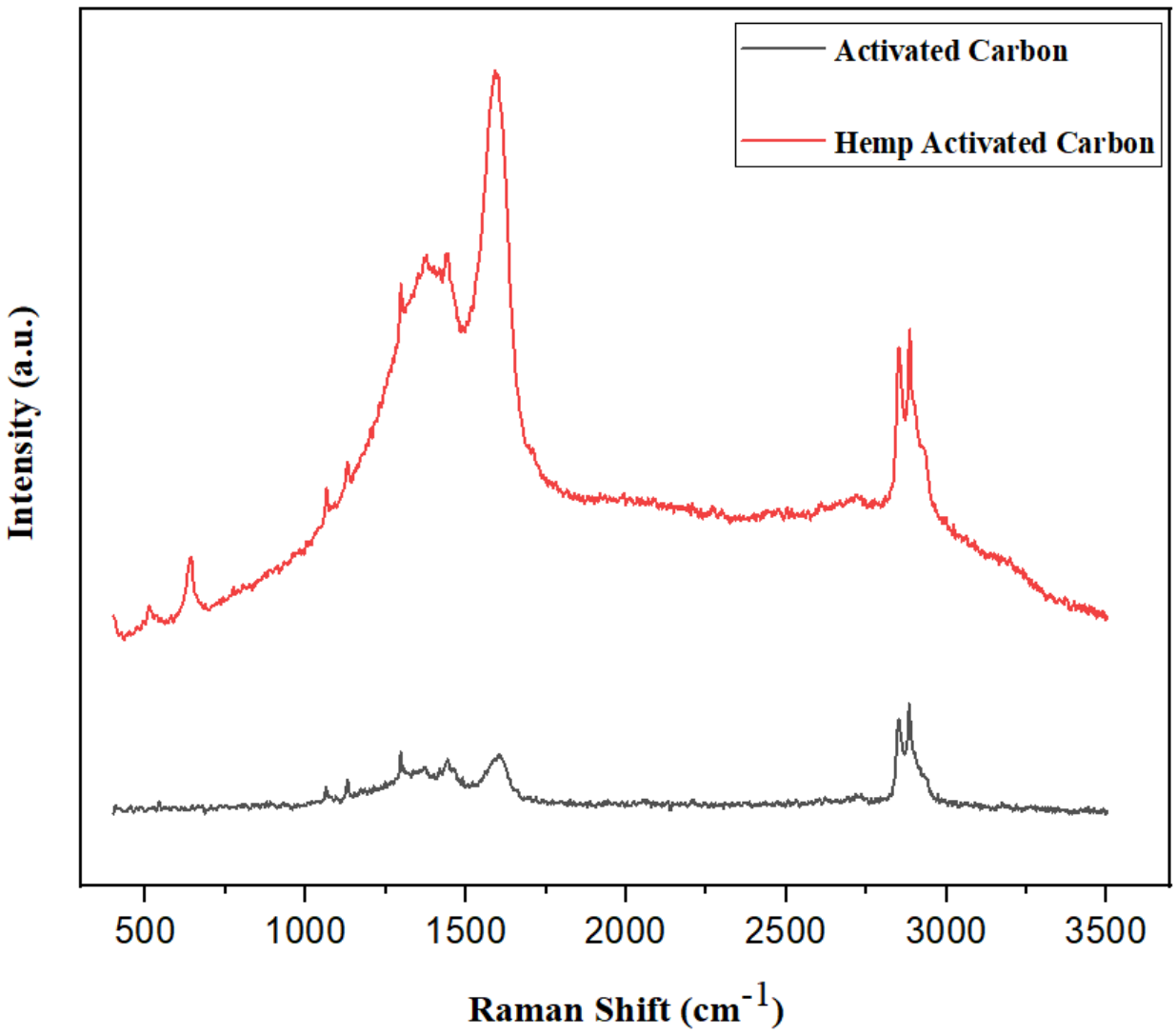

Figure 4-1 Raman spectrum of hemp derived activated carbon and commercial activated carbon

The G band corresponds to the first-order scattering and is related to the vibration of sp2-bonded carbon atoms. It usually rises in highly ordered carbon structures like graphite. While on the other hand, the D band is associated with the distortion, defects, and edges in the crystal structure [6]. Although the D band is related to the degree of defects this band also appears in the ordered carbon structures. In the current study, the G band is more strong and narrow as compared to the D band thus providing proof for the more crystalline carbon material with fewer structural defects. Moreover, the ratio between the intensity between the D and G band is also used for the estimation of structuring ordering and in our case, the low ID/IG ratio suggested that hemp-

activated carbon possessed an ordered structure and is said to have a graphite-like layered structure. Table 4.1 compares the carbon structure of commercial carbon with the hemp-activated carbon (HAC) obtained from Raman spectroscopy.

Table 4.1 Comparison of Carbon Structures obtained from Raman Spectroscopy

Sample ID	Material	Carbon Structure			
		D band	G band	ID/IG Ratio	2D
AC	Commercially Activated Carbon	1296	1588	0.82	2886
HAC	Hemp-derived Carbon	1291	1596	0.81	2882

4.2 X-ray Diffraction Analysis

X-ray diffraction (XRD) is an essential technique that is used in the characterization of materials. It reveals the information related to the nature of the material either amorphous or crystalline.

Two diffraction angles at 23.1° and 43.2° are usually observed and they indicate the presence of carbon. These are the characteristic peaks of carbonaceous materials.

The large angle XRD patterns for the conventional activated carbon and hemp-based activated carbon samples are shown in figure 4.2 A large and relatively sharp peak at around 2θ 29° corresponds to the reflection plane of (002) that represents the graphite structure indicating the presence of parallel and continuous sheets of graphite. A relatively less sharp peak between 40 ° to 50 ° corresponding to crystal plane (100) is due to the honeycomb structure resulting from sp2 hybridization. Besides this, the intensity of peaks (sharpness) observed on these two diffraction peaks reflects that the sample exhibit ordered structure as was also indicated by the Raman spectroscopy [1, 7, and 16].

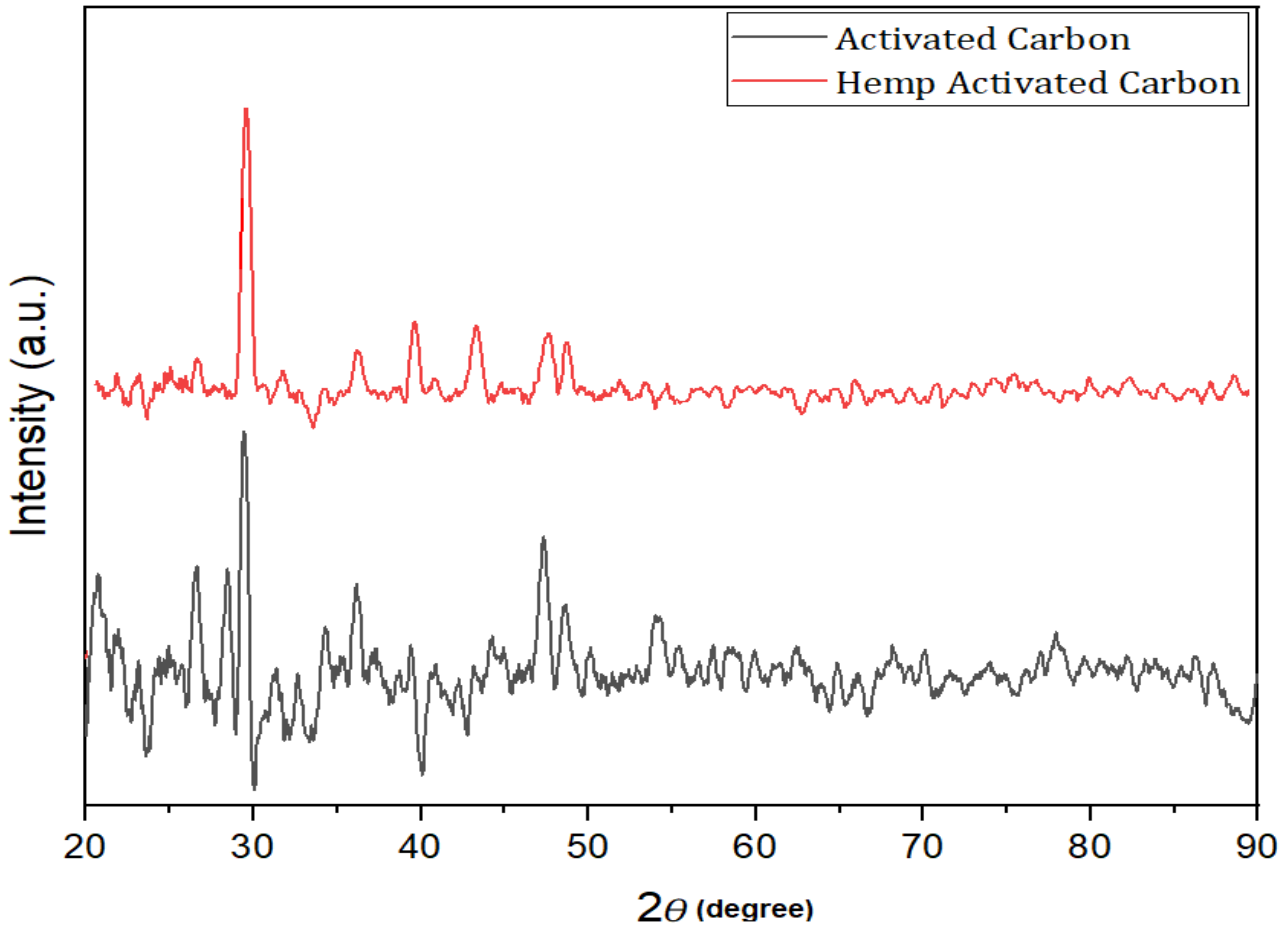

Figure 4-2 Diffraction Patterns of Conventional Activated Carbon and Hemp Activated Carbon HAC

4.3 Morphological Analysis

A material's morphology is a significant factor in determining its application. The morphology of hemp biochar and hemp-activated carbon was investigated. For this purpose Scanning electron microscope was employed to study the surface morphology. Literature suggests that when the activation is carried out with hydrogen peroxide (H_2O_2), it plays an important role in the development of pores thus improving the porosity and the surface area as it washed out all the inorganic compounds and other impurities [8].

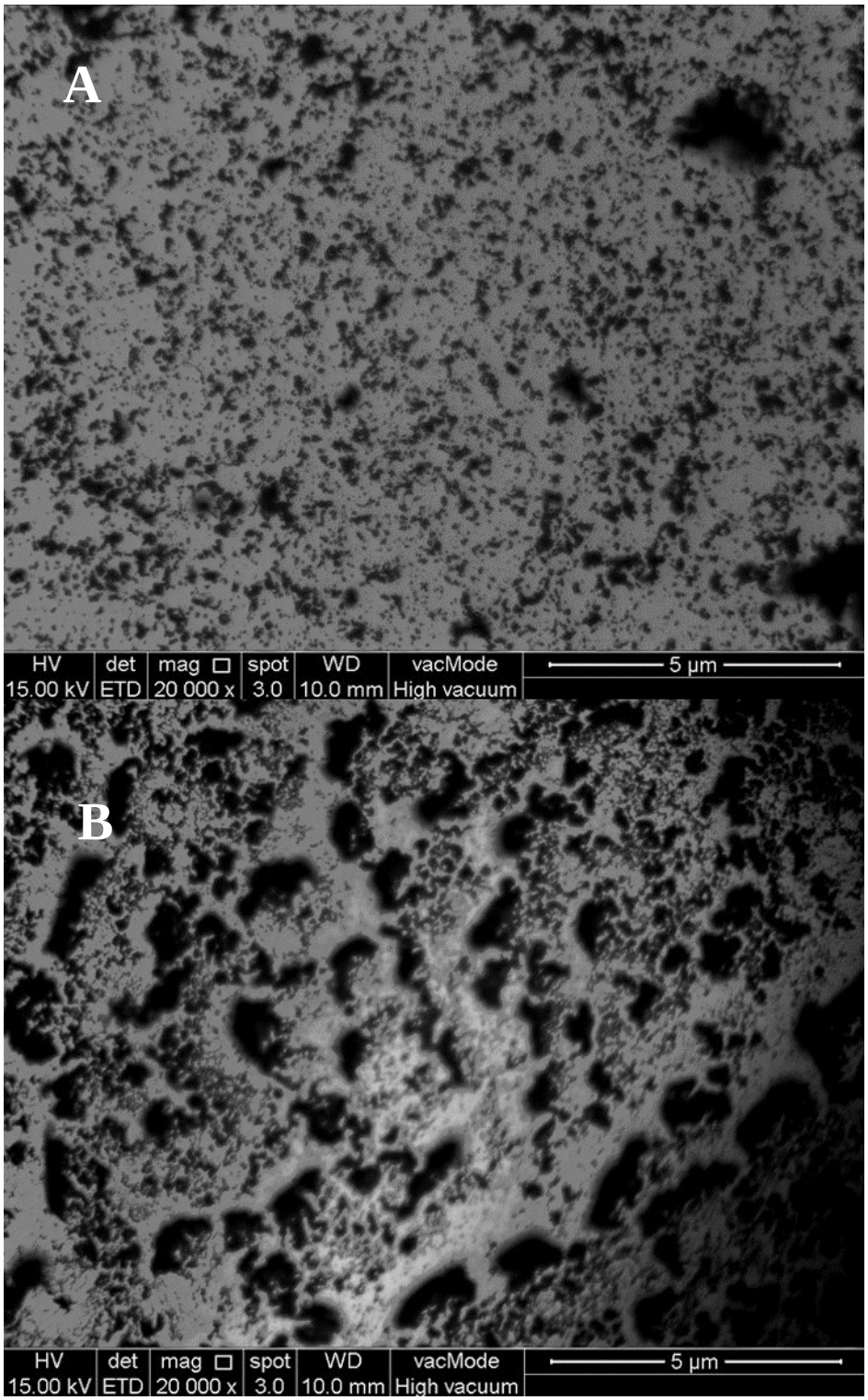

Figure 4-3 Morphological Analysis of A) Conventional carbon and B) hemp based activated carbon

The SEM images of commercially activated carbon (AC) and hemp derived activated carbon based electodes, fabricated using Doctor blade coating are shown in the figure 4.3 a) and b). The surface morphology of activated carbon derived from hemp is quite different from conventional activated carbon . In the case of conventional activated carbon, the surface is rough with irregular particles having different sizes and marked by the absence of large pores. No pores are possessed by activated carbon whereas activated carbon derived from hemp on the other hand tends to have a regular porous structure. The high surface area and mesoporosity provide more active sites thus making the HAC useful for a large number of applications including storage and adsorption of gas and for making foams, super or ultra-capacitors [1].

4.4 Fourier Transform Infrared (FTIR) Spectroscopic Analysis

For the structural elucidation, to find out the nature of functional groups and the structural bonds present in any compound, Fourier Transform Infrared Technique is used. A specific wavelength of light s used to irradiate the sample as a result of which the molecules bonded together through chemical bonds vibrate either bending or stretching at different frequencies. The frequency of light (cm^{-1}) is plotted against the intensity (either % transmission or % Absorbance) and is used to generate an FTIR spectrum. Although the materials related to activated carbons are usually composed of carbon, however, sometimes they are supposed to contain certain heteroatoms like oxygen, nitrogen, hydrogen, and sulfur thus governing the chemical and structural composition of the material [9].

Table 4-2 Fourier Transform Infrared Spectroscopy correlation table

Wavenumber (cm-1)	Vibration	Compound Class
3301	O−H	alcohol
2926	C-H	Alkane
1613	C=C	Conjugated alkene
1420	O-H	Carboxylic acid
1033	C-N	Amine
881	C-H	1,2,4 trisubstituted
717		Benzene derivatives

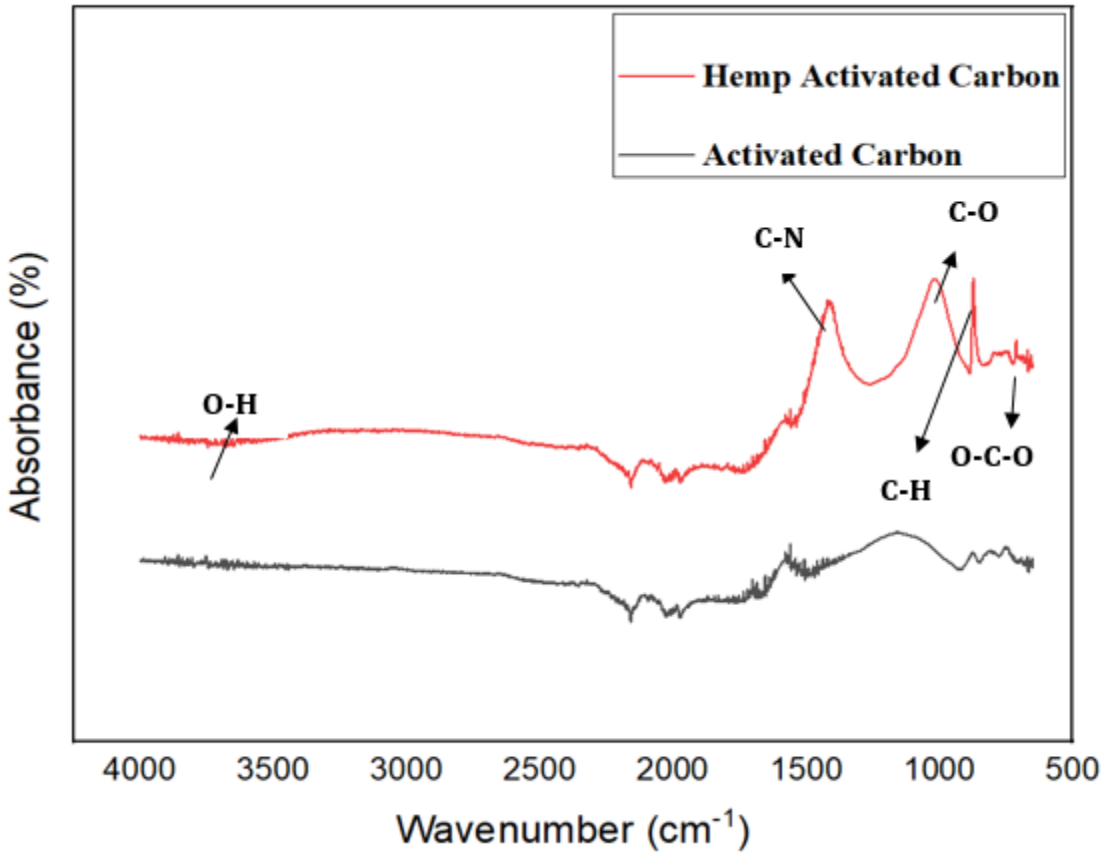

Figure 4-4 ATR-FTIR Spectra of conventional activated carbon and hemp activated carbon

As shown in figure 4.4, in the IR spectrum hemp at the top, the wave appeared from 3000 to 3600 cm^{-1}, the peak at around 3290 cm^{-1} attributed to O-H stretching of hydroxyl groups of water molecules absorbed. The peaks at 2941 and 2830 cm^{-1} are ascribed to asymmetric CH_3 and symmetric CH_2 stretching modes [1, 10, and 11]. The protein amide I gave a peak at 1630 cm^{-1} as a result of C=O stretching vibration whereas, C-N stretching of amide II along with N-H bending appeared at 1530 cm^{-1}[12]. The C-H stretching corresponding to methyl and methylene groups appeared at 2929 cm^{-1}[10]. At around 1700 cm^{-1}, a relatively weak absorbance C=O of carboxylic ester [13]. C-O stretching of alcoholic groups appeared at 1020 cm^{-1}[14]. $–CH_2$ stretching band shown at 1420 $cm^{-1.}$

Deformation vibration of surface hydroxyl groups and in-plane vibrations of C-H gave a series of overlapping absorption bands in the region ranging from 1470 to 1330 cm^{-1}. A weak band at 880 cm^{-1} is attributed to C-H out-of-plane deformation and presents a decreased monosubstituted C-H band [15].

4.5 Cyclic Voltammetry

Cyclic Voltammetry is an electrochemical technique, used for measuring the current of analysts that is redox active. It is done by scanning the potential between two or more set values in both forward and backward directions.

To study the electrocatalytic activity of as-synthesized hemp-based activated carbon counter electrode, the CV curves were recorded and compared with conventional activated carbon and conventional Pt./ITO counter electrodes and are shown in Figure 4.5.

Curves of the counter electrodes studied and the conventional Pt. /ITO counter electrodes exhibit similar behavior indicating that they tend to possess similar electrochemical properties. There are two sets of redox peaks that constitute the below curves. The following equations show the two reactions 1 and 2;

$$\mathbf{I_3 + 2e^- \rightleftharpoons 3I^-} \qquad \mathbf{(1)}$$

$$\mathbf{3I_2 + 2e^- \rightleftharpoons 2I_3^-} \qquad \mathbf{(2)}$$

The redox peaks on the left side appeared as a result of reaction 1 whereas the redox peaks on the right side were the outcome of reaction 2. Among the key functions of counter electrodes, the most important one is to act as a catalyst to carry out the reduction reaction in which tri iodide ions are converted to iodide ions thus making the left pair of redox peaks (Red 1) a critical parameter to evaluate the performance of counter electrodes [17].

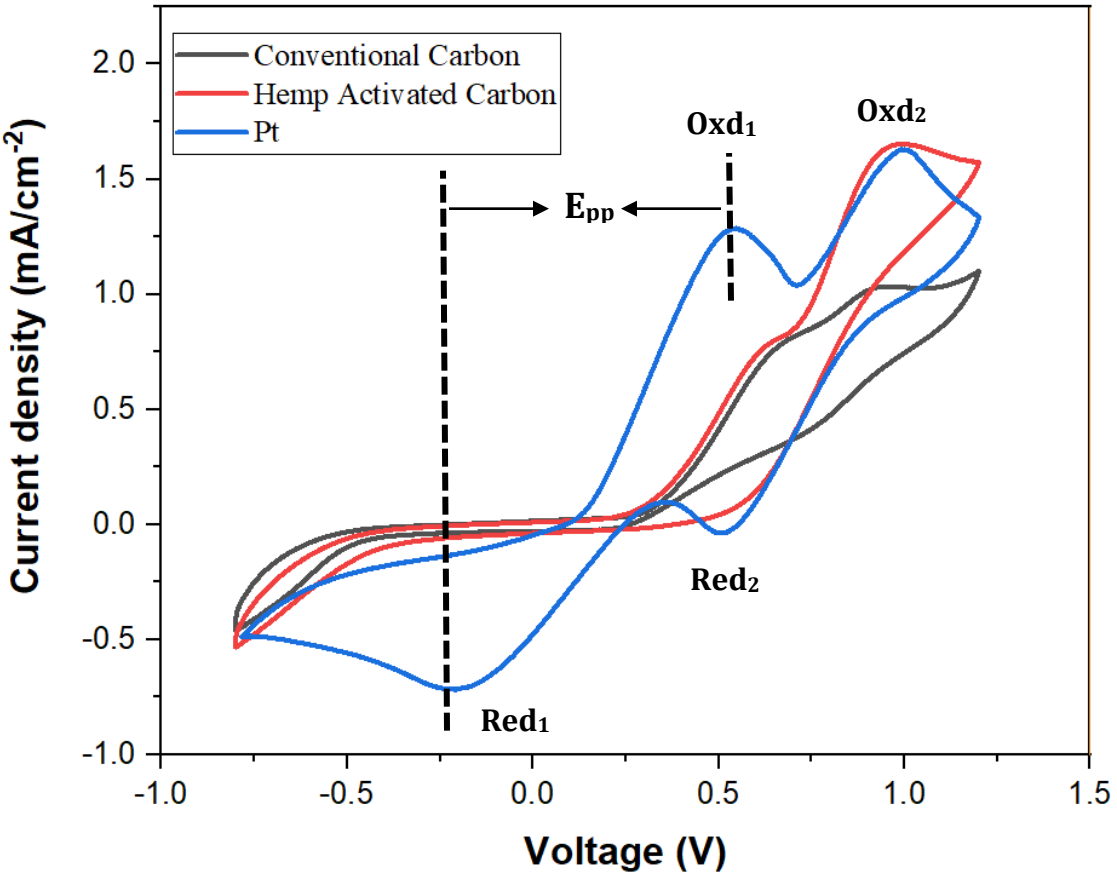

Figure 4-5 CV curves of Pt. /ITO, Conventional Activated Carbon and hemp based activated Carbon counter electrodes at scan of 100mV

In this context, for analyzing the catalytic activity of counter electrodes the peak current density is the important parameter. When a strong reaction occurs, it is indicated by the high current at a fixed voltage [18].

Peak o peak separation (E_{pp}) is another parameter for performance evaluation of counter electrodes. As a rule of thumb, generally, it is considered that the electrochemical constant (Ks) and Epp are inversely proportional. So having the smaller Epp exhibit the higher catalytic properties [19, 20]. The higher electro-catalytic activity is due to the more bonding sites which on the other hand offer rapid charge transfer thus leading to the enhancement of reaction kinetics and decreasing the I_3^- reduction over potential.

4.6 Summary

In this chapter the fabricated CEs were characterized by using various techniques. First of all, the phase identification of the CEs were detected by XRD. The elemental composition and morphology of the fabricated CE thin films were checked through the SEM. The presence of the porous carbon also support to find out the intensity peaks at specific wavelengths. To check the conductivity and electrochemical activity of the CE were tested through the cyclic voltammetry technique, that shows the oxidation and reduction peaks that are in comparison with the Pt CE.

4.7 References

[1]. M.Z. Hossain, W.W.William Z.Xu, M.B.I. Chowdhury, A.K. Jhawar, D.Machin and P.A. Charpentier, High-Surface Area Mesoporous Activated Carbon from Hemp Bast Fiber Using Hydrothermal Processing, C Journal of Carbon Research, 2018, 38(4), 1-15.

[2]. J.M-Wharry, M.M-Harris and K. Pickering, Carbonization of biomass-derived chars and the thermal reduction of a graphene oxide sample studied using Raman spectroscopy, Carbon, 2013, 59 (1), 383-405.

[3]. W. Peng, H. Li, Y. Liu and S.Song, Charczcterisation of Reduced Graphene Oxides Prepared from Natural Flaky, Lump and Amorphous Graphites. Material Research Bulletin, 2016, 78 (1), 119-127.

[4]. L. Marrot, K. Candelier, J. Valette, C.Lanvin, B. Horvat, L. Legan and D.B. Devallance,Valorization of Hemp Stalk Waste Through Thermochemical conversion for Energy and Electrical Applications. Waste and Biomass Valorization, 2022, 13 (1), 2267-2285.

[5] R. Escribano, J.J. Sloan, N. Siddique, N. Sze and T. Dudev,Raman Spectroscopy of Carbon-containing particles, Vibrational Spectroscopy, 2001, 26(2),179-186.

[6]. D.G. McCullcoh, S. Prawer and A. Hoffman, A Structural Investigation of Xenon-ion-beam-irradiated Glassy Carbon, Physical Review B, 1994, 50(1), 5905-5917.

[7]. L. Zou, L. Li, H. Song and G Morris, Using Mesoporous Carbon Electrodes for Brackish Water Desalination, Water Research, 2008, 42 (8-9), 2340-2348.

[8]. B. Shen, Z. Liu, H. Xu and F. Wang, Enhancing the absorption of elemental Mercury using Hydrogen Peroxide Modified Bamboo Carbons, Fuel, 2019, 235(1), 878-885.

[9]. S.M. Yakout and G. Sharaf ul Deen, Characterization of Activated Carbon Prepared by Phosphoric Acid Activation of Olive Stones, Arabian Journal of Chemistry, 2016, 9 (2), S1155-S1162.

[10]. J. Zhang, J. Gao, Y. Chen, X. Hao and X. Jin, Characterization, Preparation, and Reaction Mechanism of Hemp Stem based Activated Carbon, Results in Physics, 2017, 7(1), 1628-1633.

[11]. Y. wang, R.Yang and Z. Zhao, Hydrothermal preparation of highly porous carbon spheres from hemp (Cannabis sativa L.) stem hemicellulose for use in energy-related applications, Industrial Crops and Products, 2015, 65 (1), 216-226.

[12]. F. Siano, S. Moccia, G. Picariello, G. L. Russo, G. Sorrentino, M. D. Stasio, F.L. Cara and M.G.Volpe, Comparative Study of Chemical, Biochemical Characteristic and ATR-FTIR Analysis of Seeds, Oil and Flour of the Edible Fedora Cultivar Hemp (Cannabis sativa L.), Molecules, 2018, 24(1), 83.

[13]. D. Dai and M. Fan, Characteristics and Performance of Elementary Hemp Fiber, Materials Science and Applications, 2010, 6(1), 336.

[14]. M.Z. Hossain, W.W.William Z.Xu, M.B.I. Chowdhury, A.K. Jhawar, D.Machin and P.A. Charpentier, High-Surface Area Mesoporous Activated Carbon from Hemp Bast Fiber Using Hydrothermal Processing, C Journal of Carbon Research, 2018, 38(4), 38.

[15]. R. Yang, G. Liu, M. Li and J. Zhang, Preparation and N2, CO2 and H2 adsorption of super activated carbon derived from biomass source hemp (Cannabis sativa L.) stem, Microporous and Mesoporous Materials, 2012, 158 (1), 108-116.

[16]. Z. Guan, Z. Guan, Z. Li, J. Liu and K. Yu, Characterization and Preparation of Nano-porous Carbon Derived from Hemp Stems as Anode for Lithium-Ion Batteries, Nano scale Research Letters, 2019, 338(14), 1-9.

[17]. V.D. Dao, S.H. Kim, H.S.Choi, J.H. Kim, H.O.Park and J.K.Lee, Efficiency Enhancement of Dye-Sensitized Solar Cell using Pt Hollow Sphere Counter Electrodes, The Journal of physical Chemistry C, 2011, 115(51), 25529-25534.

[18]. E. Ramasamy and J. Lee, Ferrocene-derivatized Ordered Mesoporous Carbon as High Performance Counter Electrodes for Dye-Sensitized Solar Cells, Carbon, 2010,48(13), 3715-3720.

[19]. V.D. Dao and H.S. Choi, Pt Nanourchins as Effient and Robust Counter Electrode Materials for Dye-Sensitized Solar Cells. ACS Applied Material Interfaces, 2015, 8(1), 1004-1010.

[20]. B. He, Q. Tang, T. Liang and Q. Li, Efficient dye-sensitized solar cells from polyaniline–single wall carbon nanotube complex counter electrodes. Journal of Material Chemistry A, 2014, 2(9), 3119–3126.

Chapter 5

Conclusions and Future Recommendations

5.1 Conclusions

Activated carbon derived from hemp leaves is used as counter electrode for dye sensitized solar cells. The activated carbon is produced from hemp Biochar that was initially obtained after the carbonization process of hemp leaves. Then this Biochar was subjected to chemical activation process and hemp activated carbon (HAC) was formed. The prepared HAC was then used to fabricate the counter electrode and then ultimately DSSC cell. All the prepared samples were subjected to various characterization techniques. All the techniques confirmed the successful preparation of activated carbon and showed that HAC samples are comparable with the commercially available activated carbon products. Moreover, the ease of its processibility, large surface area and high pore volume make it a strong candidate for a large number of applications including gas separation and absorption, solvent recovery, contaminant removal from water, wastewater treatment and as catalyst/catalyst support for energy storage and conversion processes and also found its application in ultra-capacitors/super capacitors etc. As precursor hemp is attracting significant attention as being renewable, abundant, low cost and eco-friendly thus offer scalable route for the production of activated carbon at large scale.

5.2 Future Recommendations

Being a cost effective, easy and environmental friendly DSSC have great potential to replace the conventional first generation silicon based solar cells. Right now, DSSC have achieved an efficiency of 14%, to achieve efficiency more than 14%, extraordinary measures are needed and the recommendation are outlined below.

- Carbonaceous materials with conducting polymer are promising alternative composite
- Doctor blade coating is frequently used, but it's not a systematic approach, for its fabrication a systematic approach should be used such as spin coating, screen printing and EPD coating methods
- To prepare metal based and polymer conducting CEs, hydrothermal/ in situ polymerizations methods should to be used

- Use of natural sensitizer is a cost effective approach, because ruthenium based sensitizers are quite expensive and make DSSC expensive technology.
- Multiple layers of composites of CE can further improve the electro catalytic properties of the DSSC
- Carbon allotropes more enhance the light harvesting to absorbs more light
- To develop and explore Pt free cost effective new CEs should be prioritized

Appendix A- Publication

Electrochemical and Structural Properties of Organic Carbon based Counter Electrode for Dye Sensitized SolarCells

Syed Kazim Murtaza[1], Faisal Abbas[1], Syeda Farah Naz[1], Mustafa Anwar[1], Asif Hussain Khoja[1], Sehar Shakir[1*]

[1]U.S.-Pakistan Centre for Advanced Studies in Energy (USPCAS-E), National University of Sciences & Technology (NUST), Sector H-12 Islamabad (44000), Pakistan

*Corresponding Author's Email: sehar@uspcase.nust.edu.pk

Abstract

Dye sensitized solar cells (DSSC) are the important class of solar cells that are currently gaining the attention of scientists and researchers. The replacement of platinum based counter electrode with activated carbon can make them cost effect for different energy storage and conversion processes. In this regard, the synthesis of activated carbon from biomass is of current interest towards energy sustainability. Carbonization process largely influence the properties of biomass derived activated carbon. This study encompasses the preparation of activated carbon with extremely large surface area and high porosity from hemp using chemical activation process. Initially the hemp leaves were carbonized at 750°C followed by the activation using H_2O_2. Carbonaceous counter electrode containing Hemp activated carbon (HAC) was then fabricated by Doctor Blade coating Technique on FTO glass substrate. Different characterization techniques like XRD, FTIR, SEM, Raman Spectroscopy and Cyclic Voltammetry were used. The surface morphology was examined by SEM and it shows the development of regular porous structure indicating presence of large amount of active sites. The surface functional groups like –OH, -COOH, -C=C/C-C were confirmed by FTIR. The crystalline and graphite nature of HAC was determined by Raman spectroscopy and X-ray diffraction technique. The electrocatalytic activity was checked was cyclic voltammetry. This study offers an environmental friendly procedure for the massive production of activated carbon from hemp.